Research Square

Preprints are preliminary reports that have not undergone peer review.
They should not be considered conclusive, used to inform clinical practice,
or referenced by the media as validated information.

PtoJAZ gene family analysis in Poplar 741 and insect resistance identification for PtoJAZ10

Mengying Sun
Hebei Agricultural University
Lijiao Gu
Hebei Agricultural University
Lianxiang Long
Hebei University of Engineering
Xinghao Chen
Hebei Agricultural University
Shijie Wang
Hebei University of Engineering
Chunyu Wang
Hebei Agricultural University
Min Jiang
Hebei Agricultural University
Jun Zhang
zhangjunem@126.com
Hebei Agricultural University
Minsheng Yang
Hebei Agricultural University

Research Article

Keywords: Poplar 741, Nicotiana tabacum, JAZ gene family, PtoJAZ10 gene, Feeding insect stress, Transcriptome analysis

Posted Date: July 27th, 2026

DOI: https://doi.org/10.21203/rs.3.rs-9880715/v1

License: This work is licensed under a Creative Commons Attribution 4.0 International License.
Read Full License

Additional Declarations: No competing interests reported.

Version of Record: A version of this preprint was published at BMC Plant Biology on October 27th, 2026. See the published version at https://doi.org/10.1186/s12870-026-10170-z.

Title: *PtoJAZ* gene family analysis in Poplar 741 and insect resistance identification for *PtoJAZ10*

Mengying Sun[a,b,c†], Lijiao Gu[a,b†], Lianxiang Long[d], Xinghao Chen[e], Shijie Wang[d], Chunyu Wang[a,b], Min Jiang[a,b], Jun Zhang[a,b*], Minsheng Yang[a,b*]

[a]Forestry College, Hebei Agricultural University, Baoding 071000, China

[b]Hebei Key Laboratory for Tree Genetic Resources and Forest Protection, Baoding 071000, China

[c]State Key Laboratory of Tree Genetics and Breeding, Key Laboratory of Tree Breeding and Cultivation of State Forestry Administration, Research Institute of Forestry, Chinese Academy of Forestry, Beijing 100091, China

[d]School of Landscape and Ecological Engineering, Hebei University of Engineering, Handan 056038, China

[e] Shandong Key Laboratory of Eco-Environmental Science for the Yellow River Delta, Shandong University of Aeronautics, Binzhou 256603, China

*** Corresponding Authors:**

Jun Zhang: zhangjunem@126.com

Minsheng Yang: yangms100@126.com

Highlights:

• *PtoJAZ10* is strongly induced by insect herbivory in poplar 741

• Heterologous overexpression of *PtoJAZ10* in tobacco enhances resistance to *Helicoverpa armigera*.

• *PtoJAZ10* may enhance insect resistance by upregulating **MPK3/6**, *4CL*, and *CCoAOMT1*.

Abstract

Jasmonate ZIM-domain (JAZ) proteins are core components of the jasmonic acid signaling pathway, playing key roles in plant growth, development, and stress responses. In this study, we identified 39 *JAZ* family members in poplar 741 and designated them *PtoJAZ1* to *PtoJAZ39* according to their chromosomal order. Phylogenetic analysis grouped them into six distinct subclades, with most members harboring conserved C-terminal motifs, including motifs 1–3. Collinearity and promoter analyses revealed a close evolutionary relationship with the *Eucalyptus grandis* JAZ family, alongside an enrichment of hormone- and stress-responsive cis-elements. *PtoJAZ10* was strongly transcriptionally induced by methyl jasmonate (MeJA), abscisic acid (ABA), and *Helicoverpa armigera* feeding, with its expression increasing 17.5-fold after 24 h of herbivory, prompting its selection for further functional study. Subcellular localization confirmed that *PtoJAZ10* is a nuclear protein. Overexpression of *PtoJAZ10* in tobacco significantly reduced leaf consumption by *H. armigera* and impaired larval growth. Upon insect challenge, transgenic plants displayed markedly higher endogenous levels of JA and ABA, increased lignin accumulation, and enhanced activities of the antioxidant enzymes SOD, POD, and CAT, as well as phenylalanine ammonia-lyase (PAL), while showing lower malondialdehyde (MDA) content compared to wild-type plants. Transcriptome profiling further suggested that *PtoJAZ10* may synergistically bolster insect resistance and stress tolerance by modulating key genes within the MAPK signaling pathway (e.g., *MPK3/6*) and the phenylpropanoid biosynthesis pathway (e.g., *CCoAOMT1* and *4CL*). Collectively, our findings provide a foundation for understanding the role of *PtoJAZ10* in poplar defense mechanisms against insect herbivory.

Keywords: Poplar 741; *Nicotiana tabacum*; *JAZ* gene family; *PtoJAZ10* gene; Feeding insect stress; Transcriptome analysis

1. Introduction

JAZ proteins are plant-specific zinc finger proteins [1] widely distributed across terrestrial plants, from lower bryophytes to higher dicotyledons, and play a crucial role in induced plant defense responses[2]. Initially identified in *Arabidopsis thaliana* , JAZ proteins are classified as members of the TIFY family. A typical JAZ protein contains three domains: Jas, ZIM, and NT[3-5]. The core regulatory components of the JA signaling pathway are JAZ proteins[6]. Under resting conditions, JAZ proteins interact with adaptor proteins such as TPL (TOPLESS) to form a transcriptional co-repressor complex. By recruiting chromatin modifiers like histone deacetylases (HDAs), this complex suppresses the expression of downstream defense genes[1, 7, 8]. When plants encounter stress, endogenous JA levels increase, triggering the SCF^{COI1} complex to recognize JAZ proteins via the Jas domain and mediate their ubiquitination and degradation. This process releases inhibited transcription factors, such as *MYC2*, thereby activating the expression of early defense genes and initiating resistance responses[9, 10]. Studies have also shown that silencing JA-Ile hydroxylase to elevate endogenous JA-Ile levels can effectively enhance potato resistance to the generalist herbivore *Spodoptera exigua*.[11]. Furthermore, JAZ proteins can interact with various transcription factors, including *WRKY*, *MYB*, and *bHLH*, to regulate plant development and stress adaptation[12-14]. Therefore, functional analysis of *JAZ* genes has become an important approach for understanding the mechanisms underlying plant stress resistance.

JAZ proteins play a central role in plant responses to abiotic stresses. For instance, overexpression of *VvJAZ13* enhances cold tolerance in *A.thaliana* and *Vitis vinifera* (grapevine) by upregulating antioxidant enzymes and cold-responsive genes such as *CBF* and *OCE1*[15]. Under saline-alkaline conditions, *OsJAZ5* and *GsJAZ2* improve tolerance in rice and soybean through JA signaling and osmotic adjustment[16, 17]. During drought, interaction between *OsbHLH148* and *OsJAZ1* enhances JA signaling and drought resistance in rice[18]. JAZ proteins also contribute to biotic stress responses. *OsJAZ9* interacts with *OsbHLH034* to increase resistance to bacterial

bligh[19], while *WRKY57* binds directly to *JAZ1* and *JAZ5* promoters, promoting their expression and modulating resistance to *Botrytis cinerea*[20]. In cotton, overexpression of *GhJAZ24* confers insect resistance and leads to sterility; the GhJAZ24d protein shows activity against both *H.armigera* and *Spodoptera frugiperda*[21]. Beyond stress adaptation, JAZ proteins regulate growth and development. Heterologous expression of *SlJAZ15* in *A. thaliana* improves plant height and leaf development while enhancing resistance to *Orobanche aegyptiaca*[22]. In secondary metabolism, *MdJAZ1* and *SlJAZ10/11* regulate anthocyanin synthesis and leaf senescence, respectively[23, 24]. Additionally, JAZ proteins interact with transcription factors such as *MYB* to influence stamen development and fruit ripening[25].

Poplar 741 is an important afforestation and economic tree species in China, valued for its wide adaptability and extensive cultivation range. However, its forestry production has been severely constrained by insect pest infestation. Currently, most insect-resistance genes applied in poplar breeding are derived from heterologous species, which presents certain limitations[26, 27]. Therefore, mining insect-resistance genes from poplar itself and activating its intrinsic defense mechanisms represent a more promising strategy for insect-resistant breeding. Nevertheless, the functions of *JAZ* genes in poplar remain poorly understood, with existing studies primarily focused on abiotic stress and pathogen responses[28-30]. Although transcriptomic data suggest that some *PtJAZ* genes (e.g., *PtJAZ3*, *PtJAZ4*) may be involved in the response to insect stress[31], their specific roles have not yet been experimentally validated. In this study, we first performed a systematic bioinformatic analysis of the *JAZ* gene family in Poplar 741 and, by integrating public transcriptome data, screened candidate *PtoJAZ* genes potentially associated with insect resistance. Subsequently, leaves of Poplar 741 were treated with MeJA, ABA, and insect feeding, and expression patterns were verified using RT-qPCR. This led to the identification of *PtoJAZ10*, whose expression was consistently upregulated under all treatments. Finally, through heterologous overexpression of *PtoJAZ10* in tobacco combined with insect-feeding assays, physiological measurements, and transcriptome analysis, we preliminarily investigated the function and molecular mechanism of *PtoJAZ10* in insect resistance.

2 Materials and Methods

2.1 Plant materials

The plant materials used in this experiment included Poplar 741(*Populus alba* × [*P. davidiana* + *P. simonii*] × *P. tomentosa*), *Nicotiana tabacum*, and *Nicotiana benthamiana*. Poplar 741 is a perennial woody plant, and its tissue-cultured seedlings were obtained by cross-breeding and maintained in vitro for long-term preservation by the Laboratory of Forest Genetics and Breeding at Hebei Agricultural University. Seeds of *N. tabacum* and *N. benthamiana* were purchased from the Tobacco Research Institute, Chinese Academy of Agricultural Sciences (Beijing, China), and were propagated and preserved in a growth chamber by the same laboratory.

2.2 Identification of *PtoJAZ* gene family members

The whole-genome data of Poplar 741 were obtained from the NGDC database (https://bigd.big.ac.cn/bioproject). JAZ protein sequences from *P. trichocarpa* [31]were used as queries, and BLASTP searches against the Poplar 741 protein database were performed using TBtools with an E-value cutoff of 1×10^{-5} to identify preliminary candidate *JAZ* genes. In parallel, we employed hidden Markov model (HMM) profiles of the TIFY (PF06200) and Jas (PF09425) domains to screen for candidate *JAZ* genes in Poplar 741 using the HMMER tool (https://hmmer.org/). The results from both approaches were merged and redundant entries were removed. Domain architectures of the candidate genes were further examined using the InterPro (https://www.ebi.ac.uk/interpro/), Pfam (http://pfam.xfam.org/), and Conserved Domain Database (CDD; https://www.ncbi.nlm.nih.gov/Structure/cdd/cdd.shtml) databases. Sequences lacking a complete Jas domain were excluded, yielding the final set of *JAZ* gene family members in Poplar 741.

2.3 Chromosome localization and collinearity analysis

For the selected *PtoJAZ* family members, chromosomal localization was conducted using the Gene Location tool in TBtools. The genome sequences of *A. thaliana*, *E. grandis*, and *Oryza sativa* were retrieved from NCBI. Subsequently,

whole-genome alignments between Poplar 741 and each of these three species were performed using the One Step MCScanX-Super Fast function. The resulting synteny relationships were visualized based on the output from the MCScanX software.

2.4 Analysis of protein motifs and conserved protein domain of the *PtoJAZ* gene family

Motif analysis of the *PtoJAZ* proteins was performed using the MEME suite (http://meme-suite.org/). Multiple sequence alignment and conserved domain analysis of the amino acid sequences of the *PtoJAZ* gene family were conducted using the ClustalW and GeneDoc tools integrated into MEGA software.

2.5 Analysis of promoter elements of *PtoJAZ* gene family

The 2000-bp region upstream of the start codon (ATG) of each *PtoJAZ* ge ne was extracted from the Poplar 741 genome using TBtools and designatedas t he promoter sequence. Putative cis-regulatory elements within these promoters were then predicted using the PlantCARE online tool (http://bioinformatics.psb.u gent.be/webtools/plantcare/html/).

2.6 Phylogenetic tree analysis of *PtoJAZ* gene family

The *A. thaliana* genome database was retrieved from NCBI. Multiple sequence alignment between the *JAZ* family members of Poplar 741 and the JAZ protein sequences of *A. thaliana* was performed using the Two Sequence Files tool in TBtools. A phylogenetic tree was constructed with the Neighbor-Joining method in MEGA software [32] and was subsequently visualized and refined using the online iTOL tool (https://itol.embl.de/).

2.7 Expression pattern of *PtoJAZ* gene

Using the transcriptome data of poplar 741[33], we analyzed the expression of *JAZ* genes in different tissues (including bud, xylem, and phloem) of poplar 741, as well as the impact of salt stress (treatment with 300 mM NaCl solution for 5–7 days) on their expression. The relevant transcriptome sequencing data are available under accession number PRJCA009569 and can be downloaded from the NGDC database (https://bigd.big.ac.cn/bioproject).Furthermore, based on transcriptome data from *P.*

deltoide[34], feeding assays were conducted by enclosing six apical leaves of the plant with mesh gauze and inoculating them with third-instar larvae of *Hyphantria cunea* (fall webworm). Leaves were collected 2 h post-inoculation, including those with approximately 1/4 or 1/8 of the leaf area consumed, along with undamaged control (CK) leaves. To analyze the expression patterns of the *JAZ* genes, amino acid sequences of the *JAZ* family members from poplar 741 were aligned with their homologs in *P. deltoides* using TBtools. Heatmaps were subsequently generated to visualize the expression profiles of these genes across the different treatment samples.

2.8 RT-qPCR expression analysis of *PtoJAZ* gene under different stress conditions

Wild-type, rooted, tissue-cultured seedlings of Poplar 741 were transplanted into pots and grown in a greenhouse. When the plants reached approximately 15 cm in height, samples were collected for tissue-specific expression analysis and stress treatments. For tissue-specific expression analysis, roots, stems, and leaves were harvested to examine the expression pattern of *PtoJAZ10*. For stress treatments, leaves were either exposed to insect feeding by inoculation with third-instar larvae of *H. cunea*, or treated with hormones by spraying with 50 mg/L jasmonic acid (JA) or 100 mg/L abscisic acid (ABA) solution. Leaf samples were collected at 6, 12, and 24 h after treatment, with untreated leaves as controls.. All collected samples were wrapped in aluminum foil, flash-frozen in liquid nitrogen, and stored at –80 °C until use. Total RNA was extracted from each sample using the Polysaccharide Polyphenol Plant Total RNA Extraction Kit (DP441, Tiangen, Beijing). RNA was reverse-transcribed into cDNA using the FastKing gDNA Dispelling RT SuperMix Kit (KR118, Tiangen, Beijing). Quantitative real-time PCR (qRT-PCR) was performed on an Agilent Mx3005P system with Talent qPCR PreMix (SYBR Green, Tiangen, Beijing). Eight genes that showed high expression levels in the transcriptome data (Section 2.6) were selected for validation. Gene-specific primers were designed using Primer 6.0 software (Tab.S1). Expression levels were calculated using the $2^{-\Delta\Delta Ct}$ method, with three biological replicates per treatment.

2.9 Subcellular localization of *PtoJAZ10*

The recombinant subcellular localization vector pROKII-GFP-*PtoJAZ10* was constructed and transformed into *Agrobacterium tumefaciens* strain GV3101. Transformed colonies were cultured on plates at 28 °C for 2 days, after which a single colony was inoculated into LB liquid medium and grown at 28 °C with shaking at 200 rpm until the optical density at 600 nm (OD_{600}) reached approximately 0.6. Bacterial cells were harvested by centrifugation at 4000 rpm for 4 min, resuspended in infiltration buffer (10 mM MES, 10 mM $MgCl_2$, 150 μM acetosyringone), and incubated at room temperature for 1 h. *N. benthamiana* plants grown under greenhouse conditions were used for infiltration. The abaxial side of fully expanded leaves was gently scratched with a needle, and the bacterial suspension was slowly infiltrated into the leaves using a syringe without a needle. Infiltrated plants were kept under low light for 2 days. For nuclear staining, a DAPI working solution was prepared by diluting DAPI stock in PBS at a 1:99 ratio. Leaf discs from the infiltrated areas were excised using a cork borer, immersed in the DAPI solution for 10–15 mins, rinsed with PBS for 10 min, and mounted on glass slides. Samples were observed and imaged using a Zeiss confocal laser scanning microscope.

2.10 Construction of the *PtoJAZ10* overexpression vector and generation of transgenic *N. tabacum* plants

The coding sequence (CDS) of *PtoJAZ10* was cloned and ligated into the pNC-Cam2304-35S overexpression vector using a Nimble Cloning kit (NC Biotech, NC001). The ligation product was transformed into *Escherichia coli* DH5α competent cells. Following PCR verification, colony screening, and sequencing, the recombinant plasmid pNC-Cam2304-35S-*PtoJAZ10* was introduced into *A. tumefaciens* strain EHA105 via the heat-shock method. Subsequently, *A.*mediated leaf disc transformation was performed on *N. tabacum* (common tobacco). The third and fourth leaves from healthy 21–28-day-old seedlings were excised, their midribs removed, and cut into small segments. The explants were immersed in an *A.* suspension (resuspended in liquid medium containing 100 μmol/L acetosyringone) for 4–6 minutes, then co-cultured in the dark for 1–2 days. After co-cultivation, the leaf discs were rinsed with sterile water

and transferred to selection medium, subcultured every 3–5 days. Once resistant shoots emerged, they were transferred to a selective rooting medium for further growth.

2.11 PCR and RT-qPCR analysis of transgenic *N. tabacum* plants

Rooted seedlings obtained in Section 2.9 were propagated and subjected to a second round of rooting induction. When adventitious roots reached approximately 1 cm in length, the plantlets were acclimatized for three days. They were then transplanted into a growth substrate consisting of garden soil, vermiculite, nutrient soil, and sand (1:1:1:1), and placed in a controlled climate chamber. To maintain humidity, the plants were initially covered with plastic film, which was gradually removed to facilitate environmental adaptation. Once the plants reached about 15 cm in height, leaf samples were collected from each transgenic tobacco line as well as from wild-type controls. Genomic DNA was extracted and used for PCR amplification to verify the presence of the target gene *PtoJAZ10* and the selectable marker gene *NPTII*, thereby confirming transgenic positive lines. To assess the expression level of *PtoJAZ10* in the transgenic lines, total RNA was extracted from leaves of each transgenic line and the wild-type control. The RNA was reverse-transcribed into cDNA, which was subsequently used for RT-qPCR analysis.

2.12 Insect feeding assay on transgenic *N. tabacum*

2.12.1 Choice feeding assay

Based on the qPCR results, three transgenic lines exhibiting high expression levels were selected for feeding assays. A petri dish of identical size lined with moistened filter paper was prepared. Fifteen healthy first-instar *H. armigera* larvae of similar size were selected for the experiment. Leaves from approximately 40-day-old greenhouse-grown plants were collected, and leaf discs of uniform size were excised from both wild-type and transgenic lines. The leaf discs were placed together in the same petri dish with the larvae. Feeding behavior was observed and photographed after 6 h and 12 h. The experiment was conducted with three biological replicates.

2.12.2 No-choice feeding assay

Leaf discs of approximately equal size were excised from wild-type and transgenic lines and placed in separate petri dishes lined with moistened filter paper. Ten

second-instar *H. armigera* larvae were introduced into each dish. Leaf samples were photographed against a white A4 background at 0 h and 12 h, and leaf area loss was quantified using Photoshop software. Each treatment included three biological replicates. For the larval growth assay, fifteen first-instar larvae were placed in individual petri dishes and provided daily with fresh leaf discs from either wild-type or transgenic plants at the same time each day. Larval length and weight were recorded at each daily refreshment time point. This experiment was also performed with three biological replicates per treatment.

2.13 Determination of physiological index related data

Leaves of wild-type and transgenic tobacco lines were collected from approximately 40-day-old greenhouse-grown plants before insect feeding, as well as 6 h after insect infestation. Collected leaf samples were immediately wrapped in labeled foil, flash-frozen in liquid nitrogen, and ground using a mortar and pestle. Three biological replicates were included for each treatment. To evaluate physiological responses of wild-type and transgenic lines to insect stress, the activities of antioxidant and defense-related enzymes as well as the contents of hormones and metabolites were measured before and after herbivory. SOD, POD, CAT, PPO, and PAL activities, together with MDA and lignin contents, were determined using commercially available assay kits (Grace Biotechnology, Suzhou, China). The levels of SA, JA, ABA, and IAA were quantified according to the manufacturer's instructions of the corresponding ELISA kits (Ruixin Biotechnology, China).

2.14 Transcriptome sequencing and analysis of transgenic tobacco plants

The second to third leaves from the top of transgenic *PtoJAZ10*-OE-2, *PtoJAZ10*-OE-6, and wild-type tobacco plants were collected, with three biological replicates per genotype. The leaf samples were submitted to Novogene Co., Ltd. for transcriptome sequencing. Total RNA was extracted from each sample using TRIzol reagent, and RNA integrity was assessed with an Agilent 2100 Bioanalyzer. Raw sequencing reads were subjected to quality filtering using fastp to obtain high-quality clean reads. The clean reads were then aligned to the reference genome using HISAT2. Based on the alignment results, transcript assembly was performed with StringTie, and gene expression levels

were quantified using RSEM. Differentially expressed genes (DEGs) were identified with thresholds of FDR < 0.05 and $|\log_2 FC| > 1$. These DEGs were subsequently subjected to Gene Ontology (GO) and Kyoto Encyclopedia of Genes and Genomes (KEGG) enrichment analyses (corrected $P \leq 0.05$). Furthermore, 12 randomly selected DEGs were validated by RT-qPCR, using the *β-actin* gene as an internal control.

3 Result

3.1 Identification and chromosomal distribution of Jaz gene family in poplar 741

Based on BLASTP and HMMER searches, 39 *JAZ* family members were identified in the genome of poplar 741 and designated *PtoJAZ1* to *PtoJAZ39*. Their amino acid lengths range from 154 to 777 aa, molecular weights from 17.7 to 84.8 kDa, and isoelectric points from 5.7 to 10.2 (Table S2). The secondary structure of *PtoJAZ* proteins is predominantly composed of random coils, accounting for 56.5% to 87.8 % of each sequence (Table S3).

poplar 741 is a triploid plant comprising three sets of chromosomes. Fig. 1A, 1B and 1C depict the chromosomal distribution of the identified *PtoJAZ* genes across these three chromosome sets. Thirty-seven *PtoJAZ* genes were randomly distributed over 29 chromosomes, with the highest number (20 genes) located on the first chromosome set. Two additional *PtoJAZ* genes were found on unanchored scaffolds. Homologous genes refer to those originating from genome duplication events and residing in different chromosome sets while occupying syntenic positions. For instance, *PtoJAZ1*, *PtoJAZ3* and *PtoJAZ4* are homologous genes residing at corresponding positions on chromosome 1 (Chr. 1) in each of the three chromosome sets. Other homologous groups include (*PtoJAZ2* and *PtoJAZ5*), (*PtoJAZ6*, *PtoJAZ7* and *PtoJAZ8*), and (*PtoJAZ9*, *PtoJAZ11* and *PtoJAZ13*).

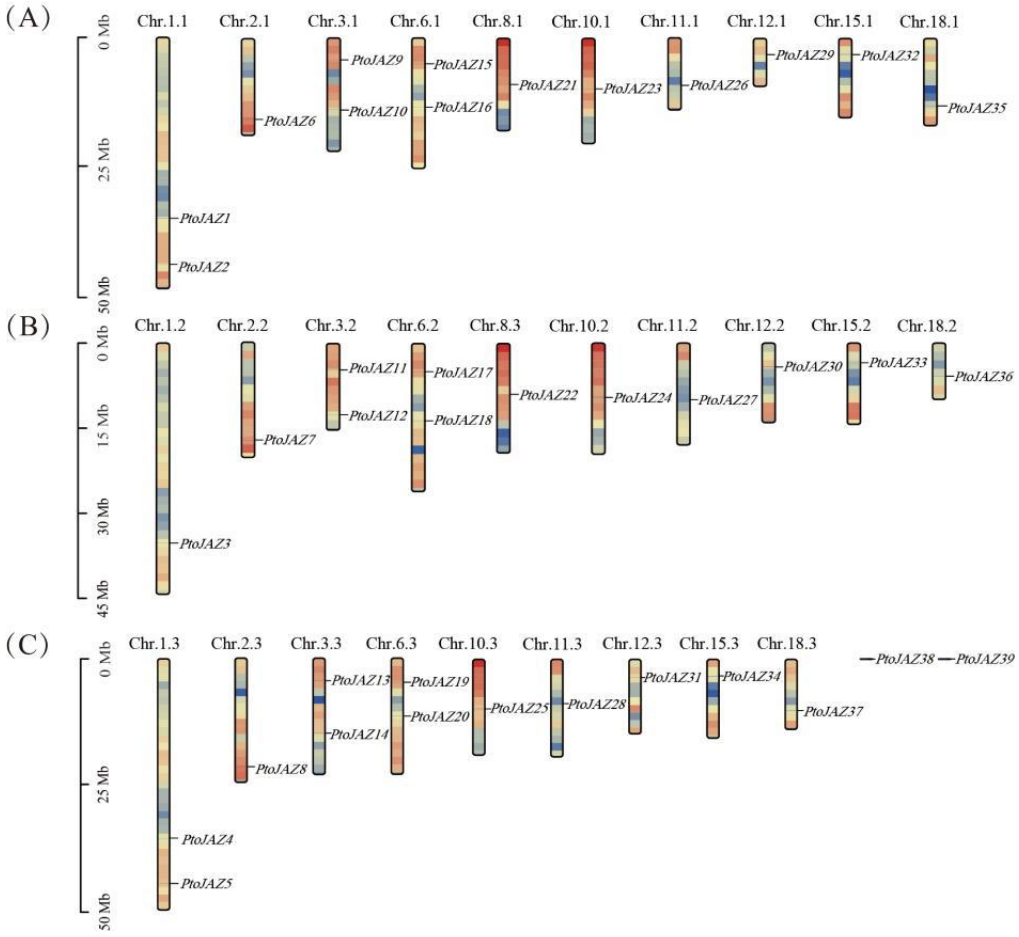


Fig. 1 Chromosomal distribution of the *PtoJAZ* gene family in poplar 741. (A–C) Chromosome sets 1, 2, and 3, respectively.

3.2 Collinearity analysis of *PtoJAZ* family members

Intraspecific and interspecific synteny analyses of the *PtoJAZ* family were conducted using the One Step MCScanX tool in TBtools. Intraspecific analysis revealed that there were 106 collinear gene pairs within poplar 741, including *JAZ4*/*JAZ9*, *JAZ1*/*JAZ19*, and *JAZ25*/*JAZ30* (Fig. 2A). Interspecific synteny was further examined between poplar 741 and three reference species: *A. thaliana*, eucalyptus, and rice (Fig. 2B). A total of 26 homologous gene pairs were identified between poplar 741 and *A. thaliana*, 17 between poplar 741 and rice, and 29 between poplar 741 and eucalyptus. These results suggest that the *JAZ* genes of poplar 741 share a closer evolutionary relationship with those of eucalyptus.

A phylogenetic tree was constructed using MEGA7.0 software, incorporating 12 *AtJAZ* genes from *A. thaliana* and 39 *PtoJAZ* genes from poplar 741 (Fig. 2C).

The *PtoJAZ* gene family was divided into six distinct groups. Group 1 contained the largest number of members, while Groups 2 and 3 contained the fewest, with only three members each. Within Group 3, the genes *PtoJAZ26*, *PtoJAZ27*, and *PtoJAZ28* formed a clade with *AtJAZ7* and *AtJAZ8*, suggesting they may share a common ancestor, participate in similar biological processes, and have retained high sequence homology and functional consistency throughout evolution.

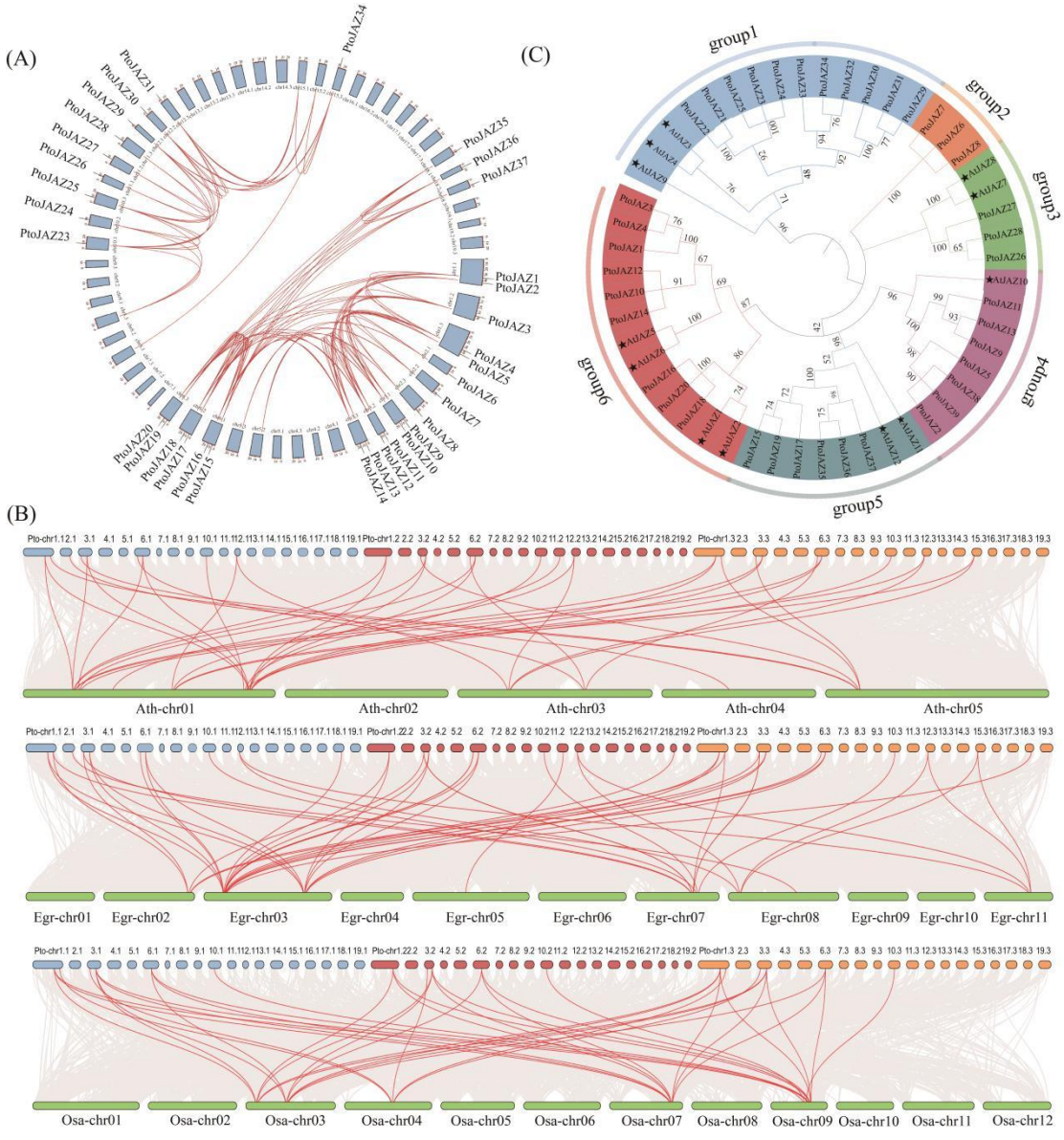


Fig.2. Synteny and phylogenetic analyses of *PtoJAZ* genes.(A) Intraspecific synteny among *PtoJAZ* genes. (B) Interspecific synteny between poplar 741 and three reference species (*A. thaliana*, *E. grandis*, and *O. sativa*). Gray lines indicate collinear regions

between genomes, and red lines highlight syntenic *PtoJAZ* gene pairs. (C) Phylogenetic tree of *JAZ* family genes from poplar 741 and *A. thaliana*.

3.3 Analysis of promoter cis-elements in the *PtoJAZ* gene family

The 2000 bp promoter regions upstream of the *PtoJAZ* gene family were analyzed using PlantCARE. Multiple types of *cis*-acting elements were identified (Fig. 3A), including light-responsive, abiotic stress-related (anaerobic induction and low-temperature responsive), and hormone-responsive elements (abscisic acid, gibberellin, auxin, methyl jasmonate, and salicylic acid). As shown in Fig. 3B, the most abundant elements were light-responsive (n = 570), ABA-responsive (n = 127), anaerobic-inducible (n = 107), and MeJA-responsive (n = 64). These results suggest that *PtoJAZ* genes may participate in plant stress responses through pathways involving light signaling, ABA, and MeJA.

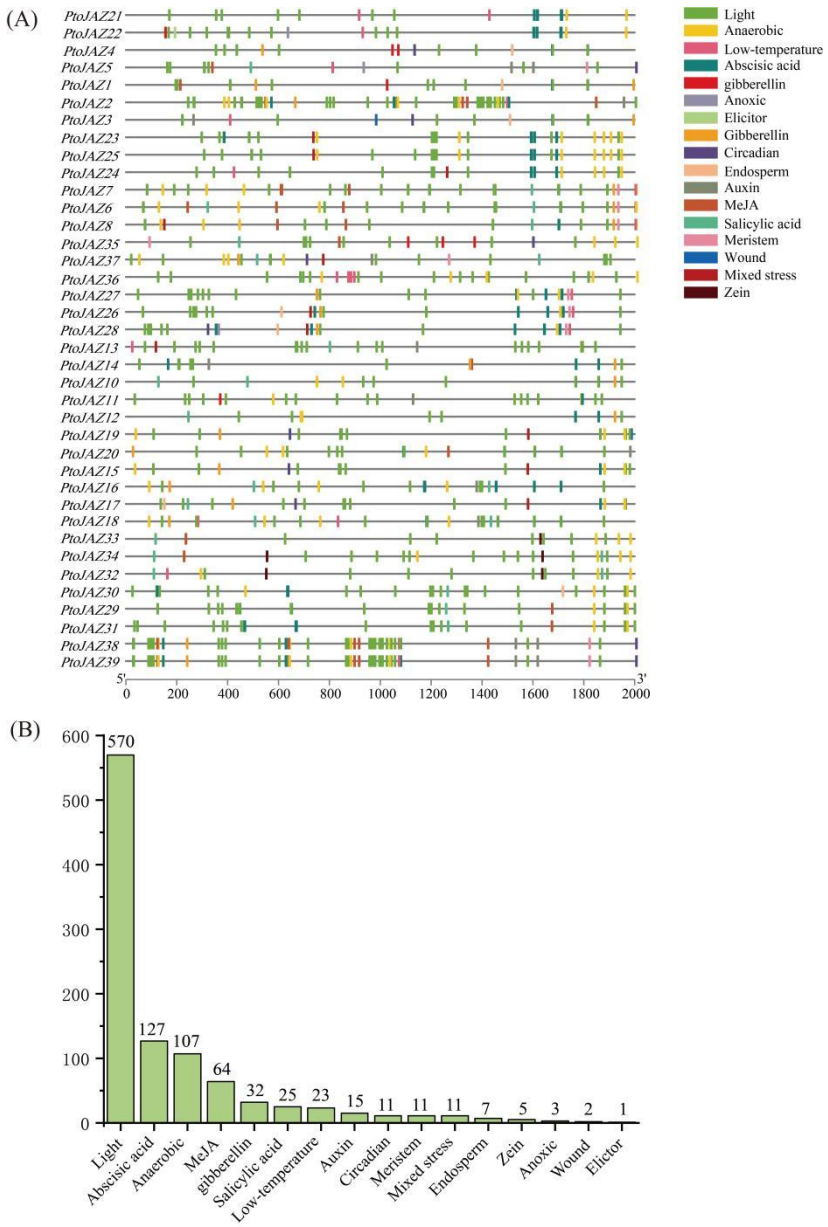


Fig.3. Analysis of *cis*-acting elements in the promoters of the *PtoJAZ* gene family. (A) Distribution of *cis*-acting elements in the promoters of *PtoJAZ* gene family. (B) Statistics on the quantity of *cis*-acting elements in the *PtoJAZ* gene family.

3.4 Expression patterns of the *PtoJAZ* gene family across different tissues and under salt or herbivore stress based on public transcriptome data

Based on public transcriptome data, we analyzed the expression patterns of the *PtoJAZ* gene family in response to insect herbivory. Homologous *JAZ* genes in Poplar 741 were identified by BLAST against the *P.deltoides* genome using TBtools. Because Poplar 741 is triploid, each *P. deltoides JAZ* gene corresponded to two or three *PtoJAZ* paralogs. As shown in Fig.4, under herbivory stre

ss, the expression levels of *PtoJAZ29*, *PtoJAZ32*, and *PtoJAZ6* were downregula ted, whereas those of *PtoJAZ15*, *PtoJAZ35*, *PtoJAZ21*, *PtoJAZ10*, *PtoJAZ1*, *Pto JAZ16*, *PtoJAZ9*, *PtoJAZ23*, *PtoJAZ2*, and *PtoJAZ26* were significantly upregulat ed, suggesting that these genes may play roles in plant defense against insect pests.

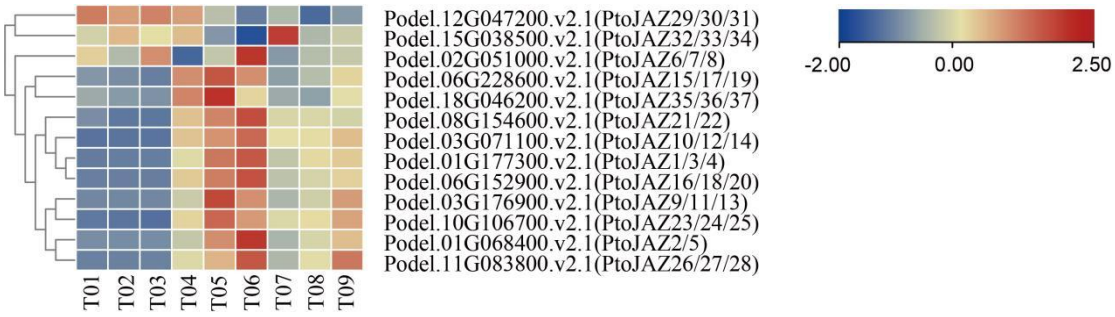


Fig.4. Transcriptome-based expression profiles of the *PtoJAZ* gene family under herbivore feeding stress. Samples T01–T03 represent untreated controls (CK); T04–T06 and T07–T09 correspond to leaf discs with approximately 1/4 and 1/8 leaf area loss, respectively, after 2 h of feeding by *H. cunea* larvae.The numbers within each group, such as T01, T02, and T03, represent biological replicates rather than distinct individual samples.

3.5 RT-qPCR analysis of *PtoJAZ* expression across tissues and under salt, drought, or herbivore stress

Based on public transcriptome data, eight *PtoJAZ* genes that exhibited signi ficantly increased expression in response to insect herbivory were selected for validation and expression profiling by RT-qPCR. The tissue-specific expression patterns are shown in Fig. 5A. Compared with leaves, *PtoJAZ1*, *PtoJAZ10*, *PtoJ AZ21*, *PtoJAZ23*, and *PtoJAZ36* were significantly upregulated in both roots and stems, suggesting that these genes may play important roles in vegetative orga ns. In addition, *PtoJAZ2* expression was upregulated in roots but showed no sig nificant change in stems or leaves. The expression pattern of *PtoJAZ26* was par ticularly distinct: it was downregulated in roots but upregulated in stems. Upre gulation of *PtoJAZ15* was specific to stem tissue. Following insect herbivory (F ig. 5B), the relative expression levels of *PtoJAZ1*, *PtoJAZ2*, *PtoJAZ10*, *PtoJAZ1*

5, *PtoJAZ21*, and *PtoJAZ23* were significantly upregulated compared with the c ontrol over the 0–24 h period. *PtoJAZ26* expression was significantly upregulate d at 6 h and 12 h, and *PtoJAZ36* was significantly upregulated at 12 h.

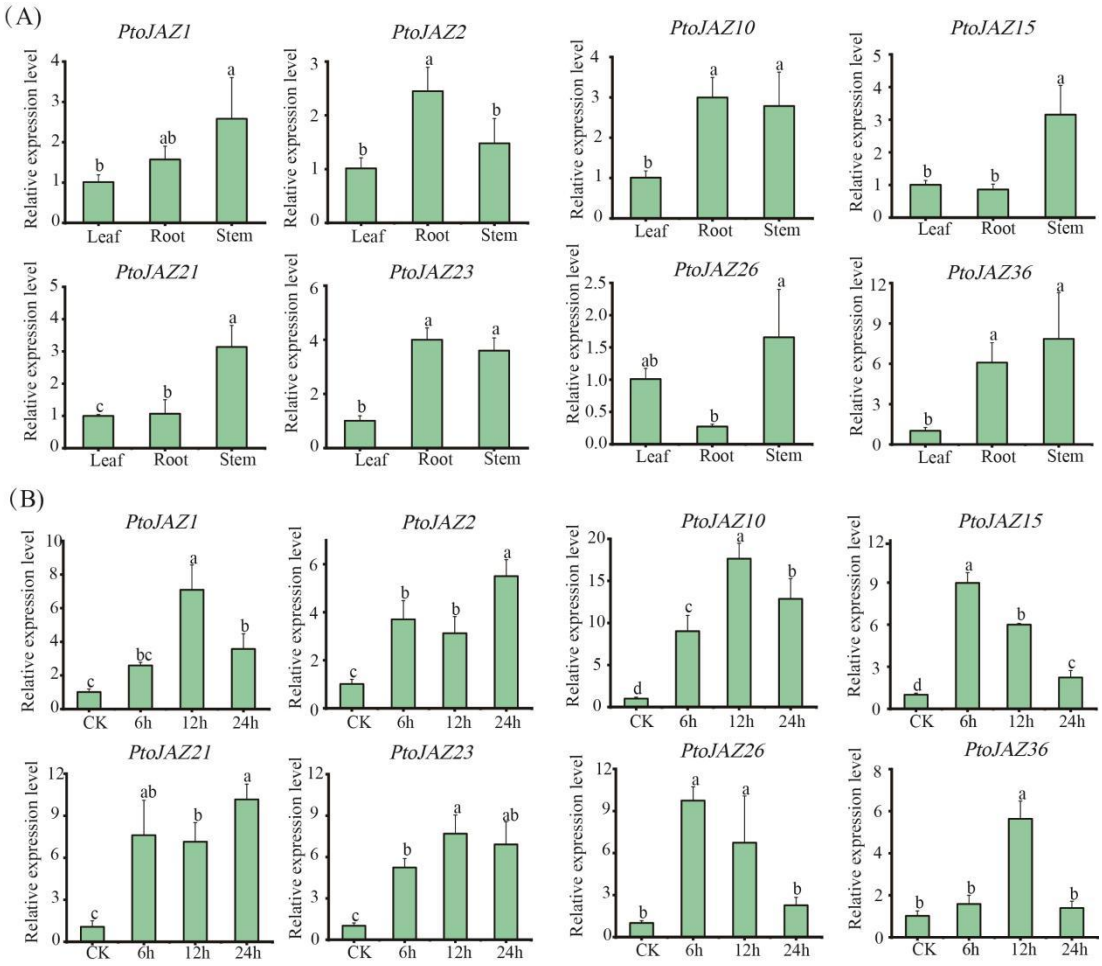


Fig.5. RT-qPCR analysis of *PtoJAZ* gene expression. (A) Expression across different tissues. (B) Expression at 6 h, 12 h, and 24 h after herbivore feeding. Data are presented as mean ± SD of three biological replicates. Different letters indicate statistically significant differences according to Duncan's multiple range test ($p < 0.05$).

3.6 RT-qPCR analysis of *PtoJAZ* expression under hormone treatments

Following MeJA treatment (Fig.6A), the expression levels of *PtoJAZ10*, *PtoJAZ15*, *PtoJAZ21*, *PtoJAZ23*, and *PtoJAZ26* were significantly elevated from 0 to 24 h compared with the control. The relative expression of *PtoJAZ1* was significantly upregulated at 24 h. *PtoJAZ2* expression initially decreased and then increased, showing significant upregulation at 12 h and 24 h. In

contrast, *PtoJAZ36* expression rose initially and then declined, with significant elevation observed at 6 h and 12 h. After ABA treatment (Fig. 6B), the relative expression levels of *PtoJAZ10*, *PtoJAZ23*, and *PtoJAZ26* were significantly upregulated throughout the 0–24 h period compared to the control. *PtoJAZ2* and *PtoJAZ36* were significantly upregulated at 24 h. The expression of *PtoJAZ1* showed a biphasic response, decreasing at 12 h before rising again at 24 h. Additionally, *PtoJAZ15* expression was significantly upregulated at 6 h and 24 h, while *PtoJAZ21* expression decreased initially and subsequently increased.

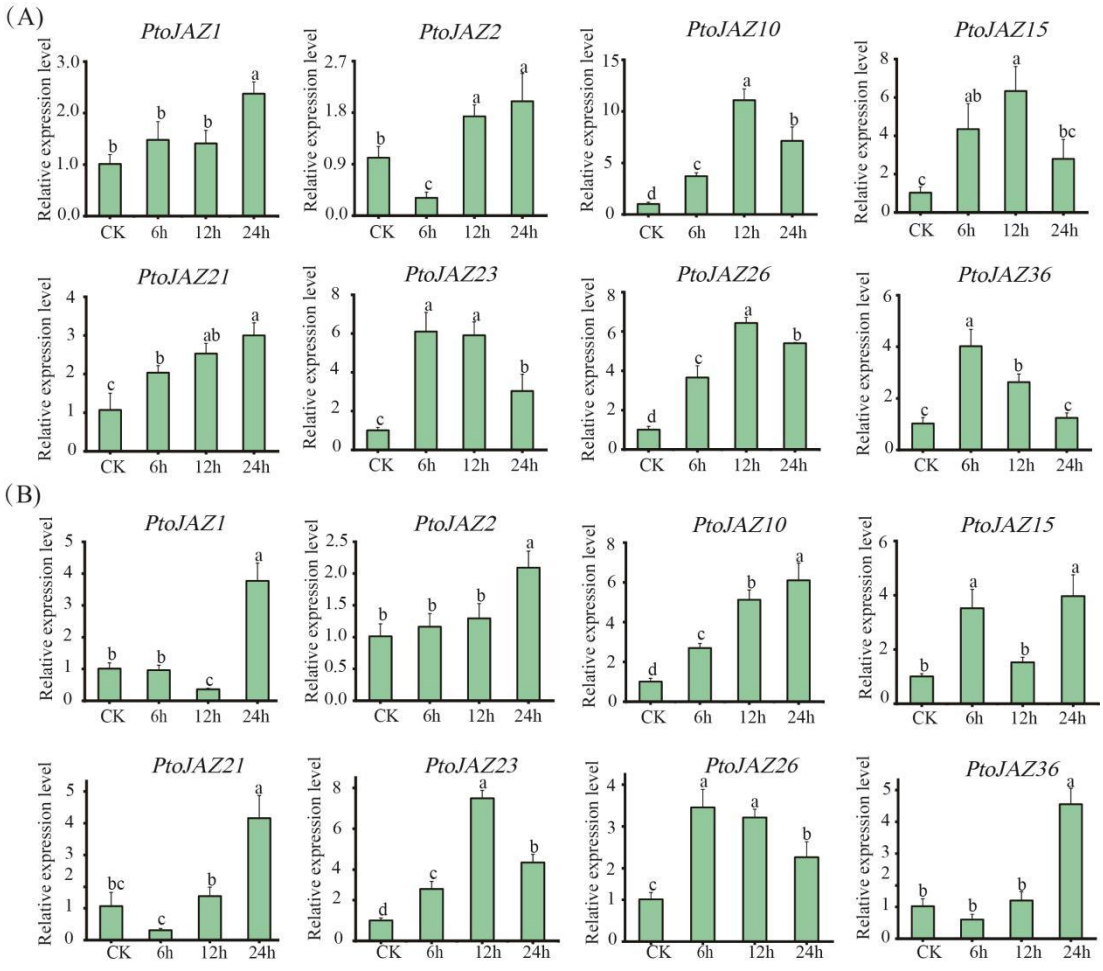


Fig.6. RT-qPCR analysis of *PtoJAZ* gene expression following hormone treatments. (A, B) Expression levels of *PtoJAZ* genes at 6 h, 12 h, and 24 h after treatment with MeJA (A) or ABA (B). Data represent the mean ± SD of three biological replicates. Different letters indicate significant differences determined by Duncan's multiple range test ($p < 0.05$).

3.7 Bioinformatics analysis and subcellular localization of the *PtoJAZ10* gene

Expression profiling indicated that the *PtoJAZ10* gene exhibited significant regulatory activity under various stress conditions, with a particularly strong response to insect defense. Therefore, this gene was selected for further functional analysis. The *PtoJAZ10* gene was cloned from poplar 741. Bioinformatics analysis of its encoded protein sequence revealed the absence of a signal peptide and a secondary structure predominantly composed of random coils (83.0%). Phosphorylation was predicted to occur mainly at serine residues (Fig. S2). Phylogenetic analysis showed that *PtoJAZ10* is closely related to proteins from *P.* species and *Salix longipennis*. All homologous proteins contained a conserved TIFY domain, and in some species (e.g., *P. alba*, *P. euphratica*), the protein also possessed a complete JAS domain (Fig. S3). The subcellular localization of the PtoJAZ10 protein was observed using a Zeiss laser confocal microscope (Fig. 7). In tobacco cells transformed with GFP alone, the green fluorescent signal was distributed throughout the cell. In contrast, in cells expressing the PtoJAZ10-GFP fusion protein, the green fluorescence was exclusively localized to the nucleus, showing complete overlap with the DAPI blue fluorescent signal. This result confirms that the PtoJAZ10 protein is nuclear-localized.

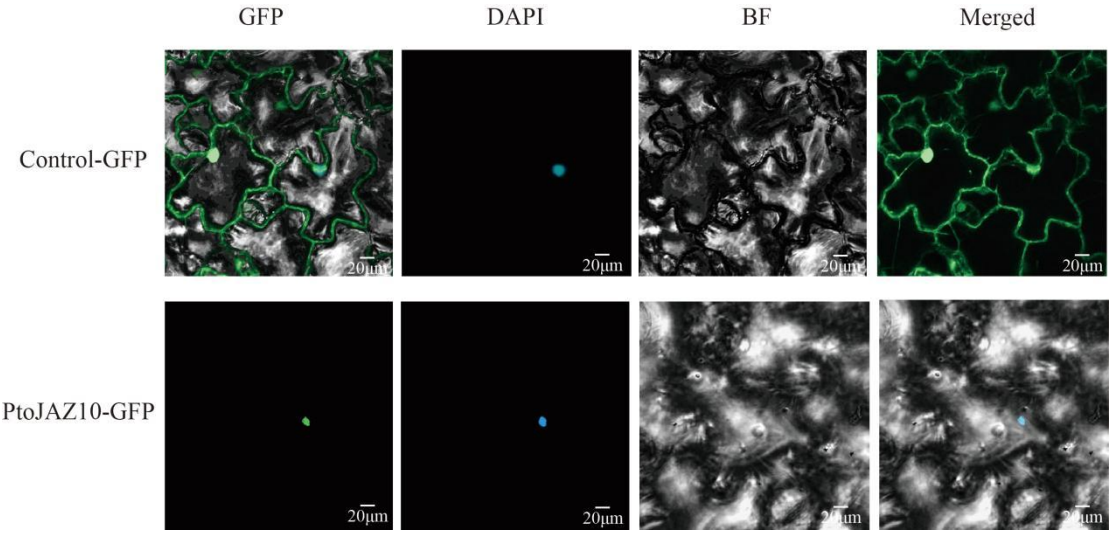


Fig.7. Subcellular localization of PtoJAZ10.The pROKII-GFP empty vector (A–D, control) and pROKII-GFP-PtoJAZ10 recombinant vector (E–H, experimental) were transiently expressed in *N.benthamiana* leaves. Shown are GFP fluorescence (green), DAPI staining (blue), bright field (BF) and merged images. Scale bar = 20 μm.

3.8 Genetic transformation and growth phenotype of *PtoJAZ10* in *N. tabacum*

The *PtoJAZ10* overexpression vector was constructed and introduced into *N. tabacum* via *Agrobacterium*-mediated leaf disc transformation. The transformation process is illustrated in Fig. 8B. PCR detection of the target *PtoJAZ10* gene and the selectable marker *NPTII* gene (Fig. 8A) yielded amplified fragments of approximately 1200 bp and 500 bp, respectively, from five independent transgenic lines, confirming successful integration of the *PtoJAZ10* transgene. RT-qPCR was then performed to assess the relative expression levels of *PtoJAZ10* in these overexpression lines (Fig. 8C). Compared with the wild-type (CK), all five transgenic lines showed significantly elevated *PtoJAZ10* expression, ranging from 4.1- to 32.5-fold higher than CK. Lines 2, 5, and 6, which exhibited the highest expression levels, were selected for subsequent functional assays. After approximately 40 days of growth in the greenhouse, plant height and stem diameter (ground diameter) were recorded and analyzed (Fig. 8D–F). Wild-type plants were generally shorter than transgenic lines, with a significant height reduction compared to lines 2 and 5, but no significant difference compared to line 6. No significant differences in stem diameter were observed between wild-type and transgenic plants.

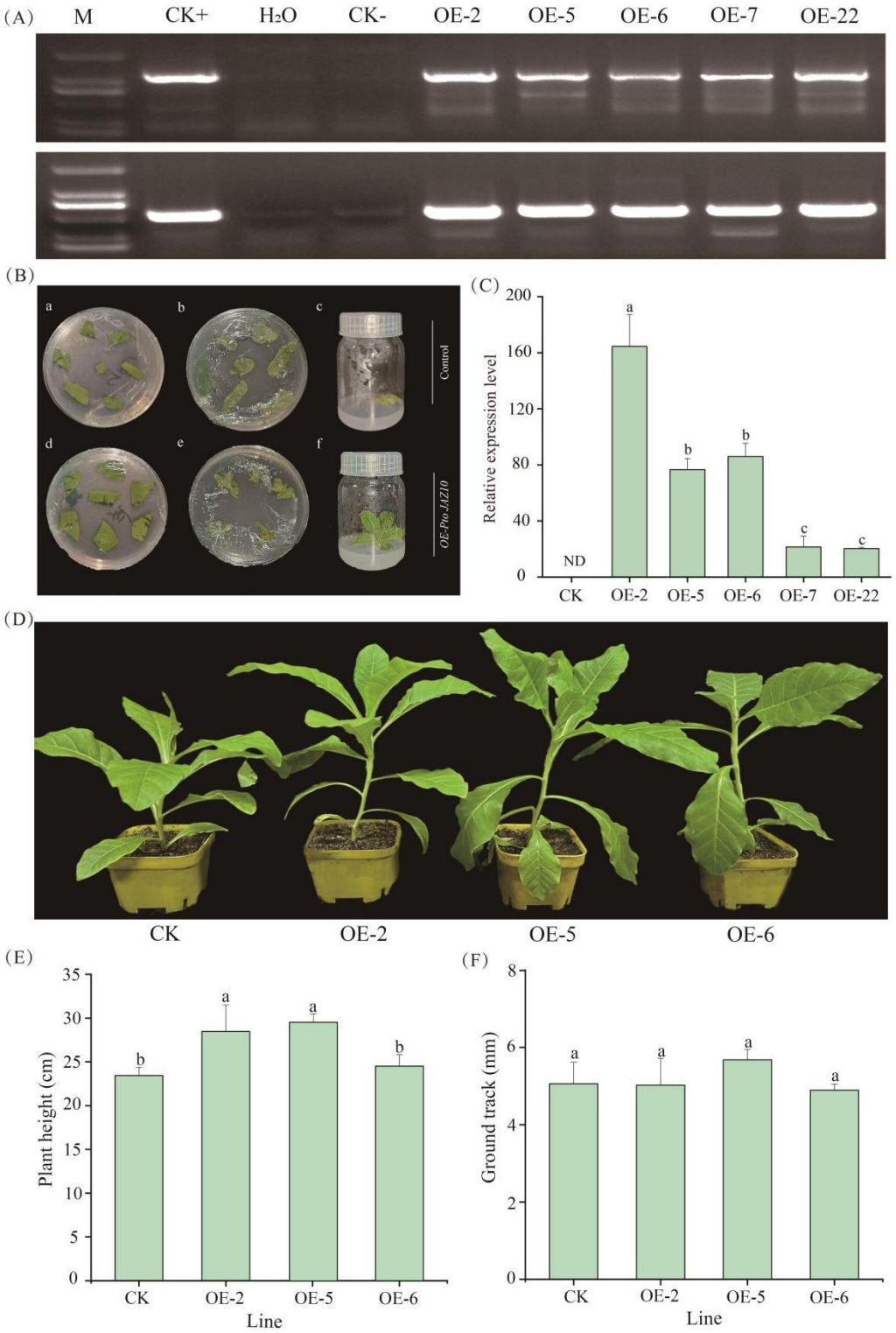


Fig.8. Genetic transformation and growth status of *PtoJAZ10*-overexpressing tobacco plants. (A) PCR detection of the 35S::*PtoJAZ10* transgene (top) and the *NPTII* selectable marker (bottom) in tobacco. M, 2000 bp DNA ladder; CK+, positive control; CK−, negative control. (B) Genetic transformation process for *PtoJAZ10* overexpression. (C) RT-qPCR validation of *PtoJAZ10* expression in

transgenic lines. No expression was detected in wild-type (CK) plants (ND). (D) Growth phenotype 40 days after transplanting. (E) Plant height. (F) Stem diameter. Data are presented as mean ± SD of three biological replicates. Different letters indicate significant differences according to Duncan's multiple range test ($p < 0.05$).

3.9 Insect feeding assay on *PtoJAZ10*-overexpressing *N. tabacum* lines

Wild-type and transgenic tobacco plants were subjected to a choice feeding assay using first-instar larvae of *H. armigera* (Fig. 9A). The results indicated that the leaf-area loss of transgenic lines was significantly lower than that of the wild-type at both 6 h and 12 h after infestation. Among the transgenic lines, lines 5 and 6 exhibited moderate leaf damage, while line 2 showed the least consumption (Fig. 9B). After 12 h of feeding, wild-type leaves suffered the most severe damage. Among the transgenic lines, leaf loss was highest in line 6 and lowest in line 2 (Fig. 9D). For the no-choice feeding assay, uniformly sized leaves from OE-2, OE-5, OE-6, and wild-type (CK) plants were placed in separate petri dishes, and larval development was monitored over a six-day period. On day 1, leaf consumption was consistently lower in transgenic lines compared to CK (Fig. 9E). Larval length after six days of feeding is shown in Fig. 9F. Larval length increased over time in both wild-type and transgenic treatments, but larvae reared on wild-type leaves were significantly longer than those fed on transgenic leaves. The changes in larval weight over the six-day period are presented in Fig. 9G. Larval weight increased gradually in the wild-type and in transgenic lines 2 and 6, while in line 5, weight increased initially but began to decline after day 4. Throughout the six-day period, larval weight was significantly higher on wild-type leaves than on any transgenic line.

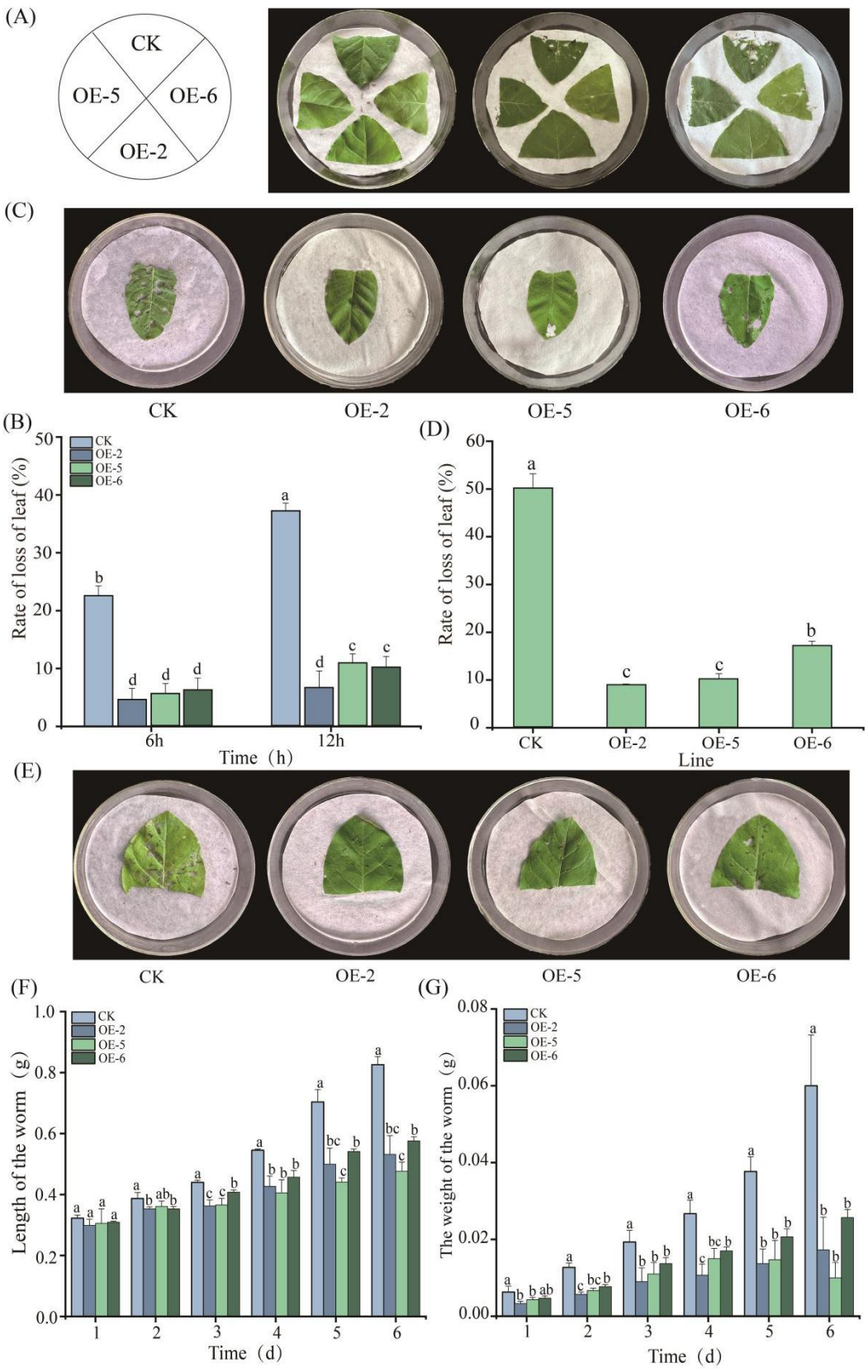


Fig. 9. Insect feeding assay on *PtoJAZ10*-overexpressing tobacco lines. (A, B) Choice feeding assay and leaf-area loss statistics. (C, D) No-choice feeding assay and leaf-area loss at 12 h. (E) Leaf damage and larval development after 1 day of no-choice feeding

by *H. armigera* larvae on wild-type and transgenic lines. (F) Larval length after 6 days of no-choice feeding. (G) Larval weight during 6 days of continuous no-choice feeding. Data represent mean ± SD of three biological replicates. Different letters indicate significant differences according to Duncan's multiple range test ($p < 0.05$).

3.10 Effects of feeding insect on physiological indexes of transgenic tobacco

Prior to *H. armigera* infestation, no significant differences in SOD and POD activities or MDA content were observed between the transgenic lines and the wild-type (CK) control, while CAT activity in the OE-5 line was lower than in other transgenic lines and CK (Fig. 10A, B). Following insect feeding, SOD and CAT activities in all transgenic lines were significantly higher than in the wild-type, with the OE-2 line showing the most pronounced increase. POD activity was also significantly elevated in transgenic plants after herbivory, particularly in lines OE-2 and OE-5 (Fig. 10A, B). Concurrently, MDA content in transgenic lines was significantly lower than in the wild-type ($p < 0.05$), with no marked differences among the transgenic lines themselves. Overall, insect infestation led to significantly higher SOD, POD, and CAT activities as well as increased MDA levels in both transgenic and wild-type plants compared to their respective uninfested controls (Fig. 10A–D).

In the absence of insect feeding, PPO and PAL activities did not differ significantly between transgenic lines and the wild-type (CK) control, while the lignin content of the OE-2 line was higher than that of other transgenic lines and CK. After herbivory, PPO activity in all transgenic lines increased significantly compared with the wild-type ($p < 0.05$), with OE-2 and OE-5 showing the most pronounced elevation. PAL activity was significantly higher in transgenic lines OE-2 and OE-6 than in CK, whereas OE-5 did not differ significantly from the wild-type. Similarly, lignin content was elevated in OE-2 and OE-6 relative to CK, with OE-5 again showing no significant difference from the wild-type control. Overall, insect infestation led to significantly higher PPO and PAL activities as well as increased lignin accumulation in both transgenic and wild-type plants compared to their respective uninfested controls (Fig. 10E–G).

In the absence of insect feeding, transgenic tobacco lines exhibited significantly higher concentrations of IAA and SA compared with the wild-type, whereas JA content

was significantly lower. No significant difference was observed in ABA levels between transgenic and wild-type plants under these conditions. Following herbivory, IAA concentrations in all transgenic lines were significantly elevated relative to the wild-type, with the OE-6 line showing the most pronounced difference. JA and ABA concentrations were also significantly higher in transgenic lines than in the wild-type after insect feeding. Among transgenic lines, ABA levels did not differ significantly from one another. SA content was significantly increased in OE-2 and OE-6 compared with the wild-type, whereas OE-5 showed no significant difference. When comparing insect-infested plants with their non-infested counterparts, both transgenic and wild-type lines displayed significantly higher JA and ABA concentrations after herbivory, while IAA concentrations were significantly lower. In transgenic lines OE-2 and OE-6, SA concentrations were also significantly elevated following insect feeding (Fig. 10H–K).

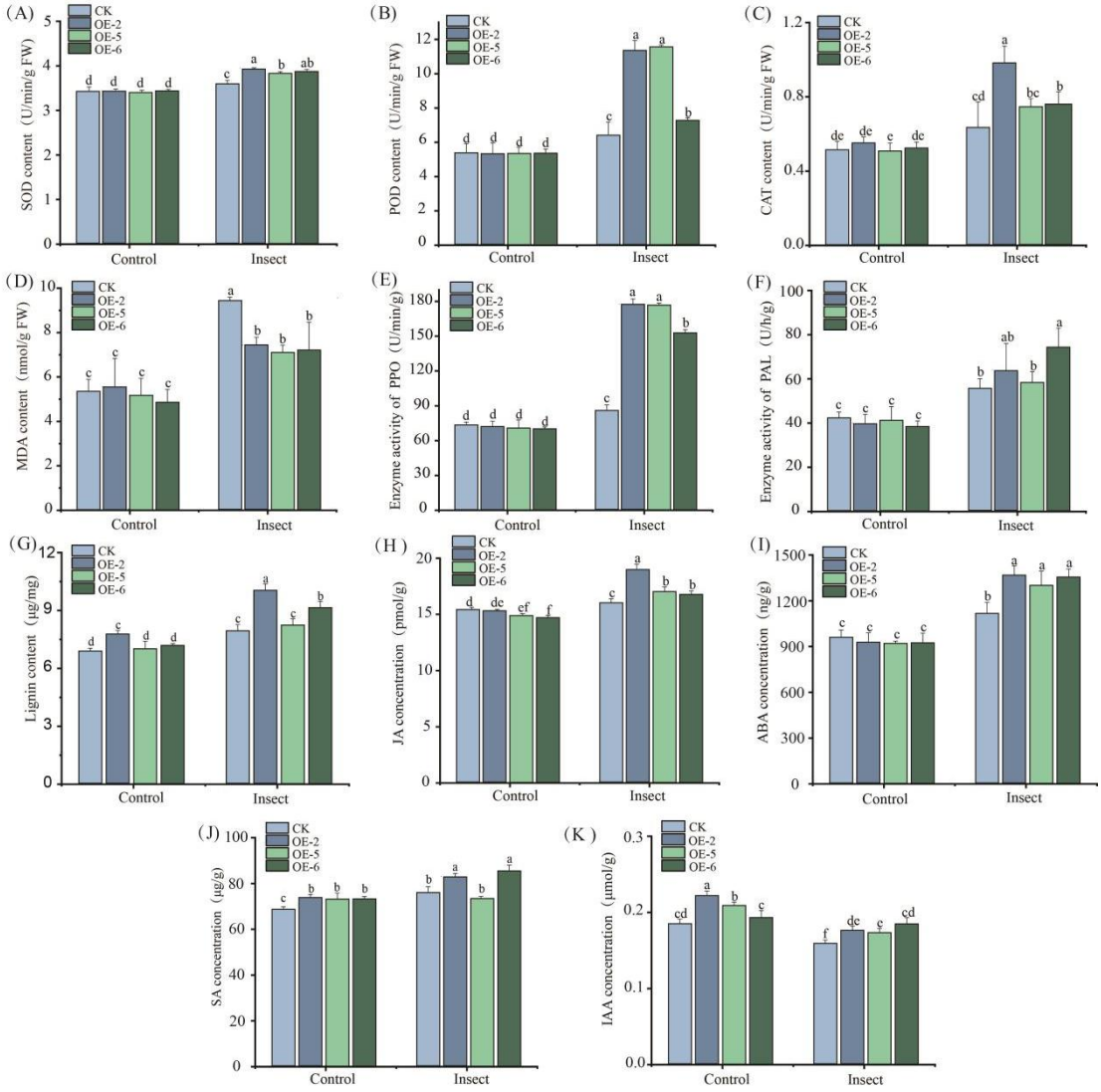


Fig.10. Analysis of physiological parameters in transgenic tobacco under insect infestation. (A) SOD; (B) POD; (C) CAT; (D) MDA; (E) PPO; (F) PAL; (G) Lignin; (H) JA; (I) ABA; (J) SA; (K) IAA. "Normal treatment" refers to the non-infested control. Data are presented as mean ± SD of three biological replicates. Different letters indicate significant differences according to Duncan's multiple range test ($p < 0.05$).

3.11 Transcriptome analysis of tobacco leaves overexpressing *PtoJAZ10*

To further elucidate the molecular mechanism underlying the insect resistance conferred by the *PtoJAZ10* gene, transcriptome analysis was performed. Among the three transgenic lines, the OE-5 overexpression line exhibited fewer differentially expressed genes (DEGs), indicating a relatively weak transcriptional response to insect stress. Therefore, to focus on the core regulatory mechanisms, the more responsive OE-2 and OE-6 lines were selected for in-depth analysis. Compared with the wild-type

control (CK), a total of 1,319 DEGs were identified in the OE-2 line, including 1,103 upregulated and 216 downregulated genes. In the OE-6 line, 1,234 DEGs were detected, comprising 631 upregulated and 603 downregulated genes (Fig. 11A). There were 1,197 DEGs unique to OE-2, 1,112 DEGs unique to OE-6, and 131 DEGs shared between the two lines (Fig. 11B). Among the commonly upregulated DEGs in OE-2 and OE-6 were genes encoding transcription factors such as *SPL*, *LPK*, *MPK3*, and *WRKY* (Fig. 11C).

In the comparative analysis between the wild-type CK and the overexpression line OE-2 (Fig. 11D), Gene Ontology (GO) enrichment showed that the Biological Process (BP) terms were predominantly associated with protein ubiquitination, exocytosis, and cell secretion. The Cellular Component (CC) terms were mainly enriched in the cell periphery, exocyst, and cell cortex. The Molecular Function (MF) terms were largely related to sequence-specific DNA binding, calcium ion binding, and ubiquitin-protein transferase activity. In the comparison between the wild-type CK and the overexpression line OE-6 (Fig. 11E), BP terms were enriched in processes such as DNA replication, ammonium transport, and L-glutamine family amino acid metabolism. CC terms were primarily associated with the cell wall and extracellular region. MF terms were enriched in catechol oxidase activity and calcium-dependent phospholipid binding.

KEGG pathway enrichment analysis was performed using a threshold of P_ value < 0.05 for significance. In the comparison between the wild-type CK and the OE-2 overexpression line (Fig. 11F), the most significantly enriched pathways included the MAPK signaling pathway – plant, sesquiterpenoid and triterpenoid biosynthesis, and phenylpropanoid biosynthesis. In the comparison between the wild-type CK and the OE-6 overexpression line (Fig. 11G), the highly enriched pathways were phenylpropanoid biosynthesis, DNA replication, flavonoid biosynthesis, arginine biosynthesis, and MAPK signaling pathway – plant. Among them, the MAPK signaling pathway and the phenylpropanoid biosynthesis pathway, which are closely associated with insect resistance, were significantly enriched in both overexpression lines.

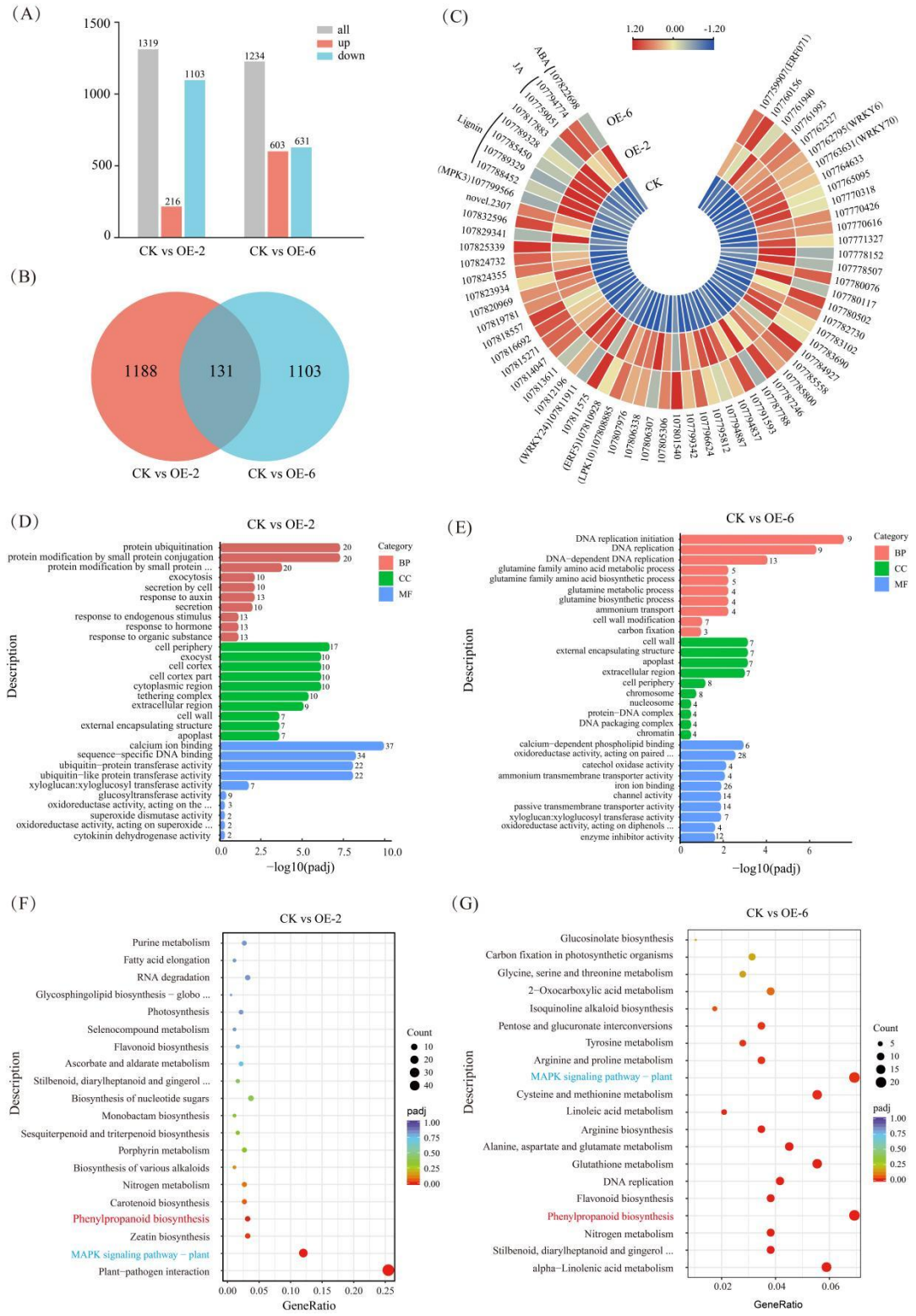


Fig.11. Differentially expressed genes (DEGs) in tobacco overexpressing *PtoJAZ10*. (A) Statistics of DEGs. (B) Venn diagram of CK vs. OE-2 and CK vs. OE-6. (C) Heatmap of transcription factors among upregulated DEGs shared by CK vs. OE-2 and CK vs. OE-6. (D) GO enrichment analysis for CK vs. OE-2. (E) GO enrichment

analysis for CK vs. OE-6. (F) KEGG pathway enrichment for CK vs. OE-2. (G) KEGG pathway enrichment for CK vs. OE-6.

3.12 MAPK signaling and phenylpropanoid biosynthesis pathways

MAPK signaling pathway contained 23 differentially expressed genes (DEGs) (Fig. 12A), many of which encode transcription factors closely associated with plant stress tolerance. Specifically, two **MPK3/6** homologs were detected in this pathway, and both were upregulated in the two overexpression lines: approximately 2.2-fold and 1.8-fold in the OE-2 line, and approximately 1.5-fold and 1.3-fold in the OE-6 line. In addition, four *WRKY33* genes were significantly upregulated in both OE-2 and OE-6, with fold changes ranging from 3.9 to 21.4 in OE-2 and from 1.9 to 5.3 in OE-6. These results suggest that *PtoJAZ10* overexpression may enhance plant defense against insects by activating key transcription factors such as **MPK3/6** and *WRKY33* in the MAPK signaling pathway.

Phenylpropanoid biosynthesis pathway contained 15 DEGs (Fig.12B), including two 4CL (4-coumarate-CoA ligase), two C4H (cinnamate 4-hydroxylase) and three CCOAOMT (caffeoyl-CoA O-methyltransferase) transcripts. Compared with the wild type, all three *CCOAOMT* genes were upregulated in both OE-2 and OE-6: *CcoAOMT1*, *CcoAOMT2* and *CcoAOMT3* were induced 5.5-, 4.4- and 10.9-fold, respectively, in OE-2, and 2.2-, 1.3- and 5.0-fold in OE-6. Moreover, two other genes in this pathway, *PNC1* and *PER51*, also showed increased expression in both overexpression lines: compared with the wild-type CK, *PNC1* and *PER51* were upregulated 2.5-fold and 1.6-fold, respectively, in OE-2, and 12.6-fold and 7.2-fold in OE-6.

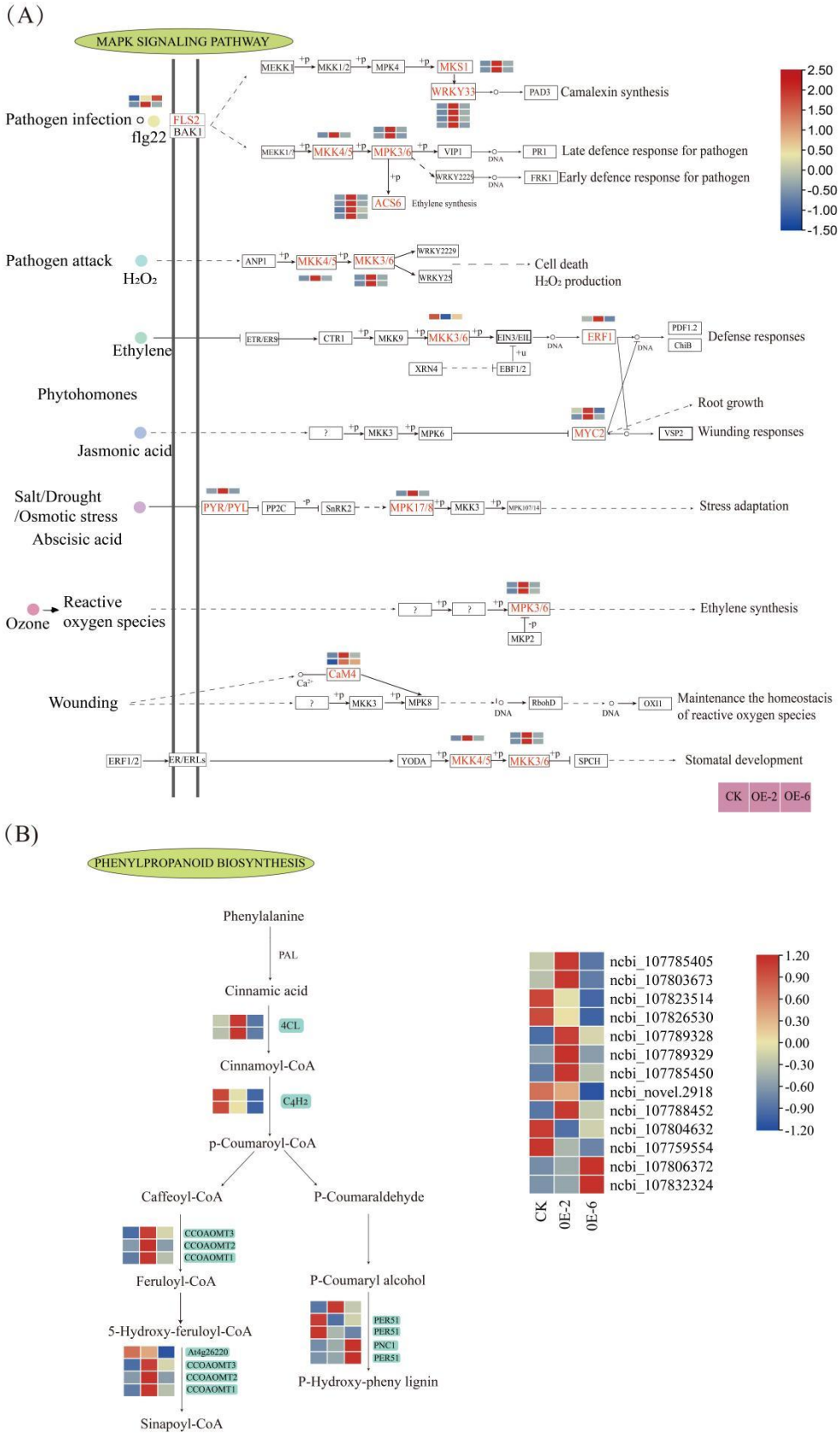


Fig.12. MAPK signaling and phenylpropanoid biosynthesis pathways. (A) MAPK signaling pathway. (B) Phenylpropanoid biosynthesis pathway.

3.13 RT-qPCR validation of differentially expressed genes

To validate the transcriptome data, the expression patterns of 12 randomly selected genes were examined by RT-qPCR. As shown in Fig.13, the expression trends of these genes were consistent with the RNA-seq results, confirming the reliability of the sequencing data.

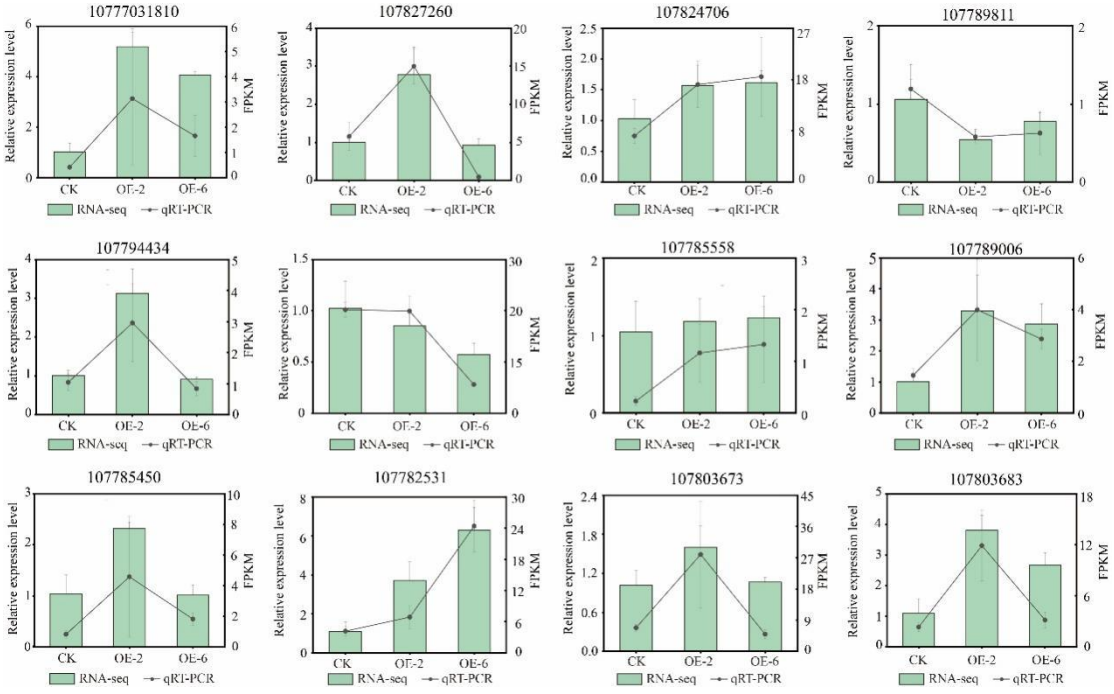


Fig.13. RT-qPCR validation of RNA-Seq-selected genes. Data are presented as mean ± SD of three biological replicates. Different letters indicate significant differences according to Duncan's multiple range test ($p < 0.05$).

4 Discussion

4.1 *PtoJAZ* gene family bioinformatics analysis

In this study, 39 *PtoJAZ* genes were identified in poplar 741, which differs from the number of *JAZ* genes (10–30) in most diploid and polyploid plants. [35, 36]. Although poplar 741 is triploid, its complement of 39 *JAZ* genes is not simply three times that of its diploid relatives (e.g., 13 genes in other poplar species)[31]. Moreover, these genes are unevenly distributed across its three homologous chromosome sets (Fig. 1), suggesting that the expansion of the *JAZ* gene family is not directly linked to genome ploidy but is likely associated with species-specific evolution and functional diversification. Collinearity analysis further indicated that poplar 741 shares the

599 greatest number of syntenic *JAZ* genes (29) with *E.* grandis (Fig. 2B), supporting a
600 closer evolutionary relationship among woody species[31]. Members of
601 the *PtoJAZ* gene family generally exhibit similar motif compositions and gene
602 structures, reflecting a common evolutionary origin. However, variations exist even
603 within the same subfamily (Fig. S1), pointing to potential functional divergence among
604 individual members.

605 Promoter analysis and hormone treatment experiments revealed that *PtoJA*
606 *Z* promoters are enriched in light-, ABA-, and MeJA-responsive *cis*-elements, an
607 d their expression was significantly induced by both MeJA and ABA (Figs. 3,
608 6A-B). These findings align with reports in sorghum [37] and radish[38], under
609 scoring the central role of JAZ proteins in integrating multiple hormonal signal
610 s to regulate stress responses. Expression analysis revealed that *PtoJAZ10* trans
611 cript levels were significantly induced by insect herbivory (Fig. 4). This result
612 was independently confirmed by RT-qPCR (Fig. 5), highlighting the likely impo
613 rtance of *PtoJAZ10* in insect defense. Subcellular localization analysis confirmed
614 that *PtoJAZ10* is nuclear-localized (Fig.7), consistent with the localization patt
615 erns reported for most JAZ proteins in petunia[39], *Toona sinensis* [35], and to
616 mato [22]. However, some studies, such as those on *Mentha haplocalyx McJAZ*
617 *2/3*[40], have reported alternative subcellular localizations, suggesting that JAZ
618 protein localization may be gene-structure dependent and could influence functi
619 onal specificity.

620 **4.2 *PtoJAZ10* enhances insect resistance in tobacco by boosting enzyme activities**
621 **and modulating hormone levels**

622 Heterologous overexpression of *PtoJAZ10* significantly enhanced the resistance
623 of tobacco to *H. armigera*. Under both choice and no-choice feeding assays (Fig. 9),
624 larvae consistently preferred wild-type tobacco leaves. The leaf-area loss in transgenic
625 lines was significantly lower (reduced by 18.1–34.3%) than in the wild-type. As feeding
626 duration extended, larvae reared on wild-type leaves grew significantly longer and
627 heavier than those fed on transgenic leaves. By the end of the 6-day assay, larval length
628 and weight on transgenic leaves were reduced by 57.8–69.7% and 16.7–42.8%,

respectively, compared to the wild-type group. These results indicated that *PtoJAZ10*-overexpressing plants likely deter *H. armigera* feeding and attenuate larval development, possibly through activation of a more efficient defense system under pest stress.

This enhanced resistance appears to involve multiple physiological and hormonal adjustments. First, transgenic lines exhibited significantly elevated activities of antioxidant enzymes (SOD, POD, and CAT) following herbivory (Fig. 10A–C), consistent with responses observed in insect-stressed transgenic impatiens[41]. This suggests a coordinated enhancement of the antioxidant system to mitigate oxidative damage by rapidly scavenging reactive oxygen species[42]. Concurrently, key defense-related enzymes (PPO and PAL) showed increased activity, lignin content rose, and the level of MDA—a marker of membrane lipid peroxidation—was relatively lower in transgenic plants (Fig. 10D–G). These changes indicated a more effective activation of the phenylpropanoid pathway, promoting the synthesis of lignin and toxic quinones that can directly inhibit insect digestion and development[43]. Second, insect feeding induced significant accumulation of JA, ABA, and SA in transgenic plants (Fig. 10H–K), aligning with hormonal shifts reported in wheat infested by Hessian fly [44] and in whitefly-infected tomato[45]. The concurrent rise in JA and ABA, together with enhanced SA signaling without suppression of the JA pathway (akin to the role of MEcPP in boosting SA-related genes while maintaining JA-responsive gene expression in *A. thaliana* [46]), suggests that *PtoJAZ10* may act upstream in a complex hormonal network, amplifying insect-resistance responses by coordinating multiple defense-hormone signals[47].

4.3 Overexpression of *PtoJAZ10* modulates the expression of stress-responsive genes in tobacco

Transcriptome analysis indicated that overexpression of *PtoJAZ10* likely modulates the expression of several stress-related genes. Among these, *MYC2*—a key transcription factor in the JA signaling pathway—was upregulated in transgenic lines, consistent with its known role in regulating growth and defense genes in tomato[48]. Moreover, multiple co-upregulated DEGs, such as *SPL* and *LPK*, have been widely

implicated in plant immune regulation, and genes associated with JA, ABA, and lignin biosynthesis also showed elevated expression (Fig. 11C). For instance, *OsSPL4* positively regulates rice resistance to blast[49], whereas *OsSPL10* negatively modulates defense against the brown planthopper[50]; wheat *LPK10* enhances resistance to leaf rust and powdery mildew[51]. The MAPK signaling cascade plays a central role in transducing extracellular stimuli into intracellular responses. In tobacco and tomato, *MPK3/6* is strongly activated upon insect feeding, thereby triggering downstream responses; notably, *MPK6* is essential for JA biosynthesis[51, 52]. In this study, *MPK3/6* genes in the MAPK pathway were upregulated in tobacco following *H. armigera* infestation (Fig. 12A). These results suggested that *PtoJAZ10* may broadly influence plant resistance to diverse biotic stresses by regulating a core set of transcription factors.

Notably, key genes in the phenylpropanoid biosynthesis pathway—*4CL* and *CcCCoAOMT1*—were significantly upregulated in transgenic plants (Fig. 12B). This pathway is central to lignin synthesis, and lignin accumulation not only reinforces cell-wall mechanical strength to form a physical barrier [53] but also yields various insect-resistant and antimicrobial secondary metabolites during its biosynthesis[54]. Previous studies have confirmed that heterologous overexpression of *Fm4CL2* [55] or *CcCCoAOMT1* [56]increases lignin content and thickens the cell wall in tobacco. Correspondingly, in this work, overexpression of *PtoJAZ10* elevated lignin content in tobacco after insect feeding (Fig. 10G). Thus, *PtoJAZ10* may enhance both physical and chemical defenses in plants by activating phenylpropanoid metabolism.

In this study, we initially confirmed that PtoJAZ10 enhances plant resistance to insects using an Agrobacterium-mediated heterologous overexpression system in tobacco. Nevertheless, tobacco (*N. tabacum*) and Poplar 741 belong to different families and genera, and substantial differences may exist between the two species in the jasmonic acid signaling pathway, secondary metabolic networks, and defense response patterns against leaf-feeding insects. Therefore, the regulatory network and physiological function of *PtoJAZ10* in its native host, poplar, may be more complex,

and the phenotypic and molecular evidence obtained from tobacco may not fully reflect its actual role in Poplar 741. To overcome this limitation, future studies will conduct homologous overexpression and RNAi/CRISPR-mediated knockdown experiments in poplar, providing more reliable evidence through direct genetic transformation to clarify the true function of *PtoJAZ10* in poplar defense against insect herbivory.

5 Conclusion

In this study, 39 *JAZ* family genes were identified for the first time in poplar 741. These genes, distributed across 29 chromosomes, were classified into six subfamilies. Phylogenetic analysis revealed a close evolutionary relationship with *Eucalyptus*. Promoter analysis indicated the presence of various hormone- and light-responsive cis-elements. Expression profiling demonstrated that multiple *PtoJAZ* genes responded to hormonal and pest stresses, with *PtoJAZ10* showing particularly strong induction. Subcellular localization confirmed that the *PtoJAZ10* protein is nuclear-localized. Functional validation showed that heterologous overexpression of *PtoJAZ10* in tobacco significantly enhanced resistance to *H. armigera*. This was associated with elevated levels of JA and ABA, increased activities of key defense enzymes (SOD, POD, CAT, PPO, PAL), and higher lignin content, collectively leading to inhibited insect growth and reduced leaf damage. At the molecular level, *PtoJAZ10* likely enhances plant insect resistance by upregulating the expression of *MPK3*, *MYC2*, and key genes in the phenylpropanoid biosynthesis pathway (e.g., *4CL*, *CcCCoAOMT1*), thereby synergistically strengthening lignin synthesis and defense signaling under pest stress.

Abbreviation

MS	Murashige and Skoog
AS	Acetosyringone
JA	Jasmonic acid
MeJA	Methyl jasmonate
SA	Salicylic acid
ABA	Abscisic acid
IAA	Indole-3-acetic acid

SOD	Superoxide dismutase
POD	Peroxidase
CAT	Catalase
PPO	Polyphenol oxidase
PAL	Phenylalanine ammonia-lyase
PBS	Phosphate-buffered saline
GO	Gene ontology
KEGG	Kyoto Encyclopedia of Genes and Genomes
qRT-PCR	Real-time fluorescent quantitative PCR

Acknowledgements

We thank the Forest Genetics and Breeding Laboratory of Hebei Agricultural University for providing the experimental facilities and technical support for this study

Authors' contributions

Mengying Sun: Methodology, Validation, Visualization, Data Curation, Investigation, Formal analysis, Writing–original draft. Lijiao Gu: Writing–original draft, Data Curation, Methodology, Visualization, Investigation, Formal analysis. Lianxiang Long: Validation, Visualization, Formal analysis. Xinghao Chen: Validation, Resources, Investigation, Data Curation. Shijie Wang: Validation, Resources, Investigation, Visualization. Chunyu Wang: Validation, Resources, Investigation, Formal analysis. Min Jiang: Validation, Resources, Investigation, Formal analysis. Jun Zhang: Conceptualization, Methodology, Funding acquisition, Supervision, Writing - Review & Editing. Minsheng Yang: Writing - Review & Editing, Conceptualization, Methodology, Funding acquisition, Supervision.

Funding

This work was funded by the Science Research Project of Hebei Education Department (grant numbe No.QN2026405) and the National Natural Science Foundation of China (grant number No.32201578).

Data availability

The datasets presented in this study can be found in online repositories. The names of the repository/repositories and accession number(s) can be found in the Genome Sequence Archive (GSA) (https://ngdc.cncb.ac.cn/gsa/GSA) under accession number CRA056445.

Declarations

Ethics approval and consent to participate

The plant materials used in this study were collected from the Hebei Key Laboratory for Tree Genetic Resources and Forest Protection, with permission from the relevant authorities. All experiments were conducted in compliance with national and international ethical guidelines for plant research. As this study did not involve human or animal subjects, no ethics approval for human or animal research was required. We confirm that the collection and use of plant samples adhered to local environmental protection regulations, and the necessary collection permits were obtained

Consent for publication

All authors have read and agreed to the content of this study and confirm that the research results have not been published elsewhere or submitted to other journals simultaneously.

Competing interests

The authors declare no competing interests

References

1. Ali MS, Baek KH. Jasmonic acid signaling pathway in response to abiotic stresses in plants.Int. J. Mol. Sci. 2020;21(2):621-640. https://doi.org/10.3390/ijms21020621.
2. Zhang L, You J, Chan Z. Identification and characterization of TIFY family genes in *Brachypodium distachyon*. J Plant Res. 2015;128(6):995-1005. https://10.1007/s10265-015-0755-2.
3. Mandaokar A, Thines B, Shin B, et al. Transcriptional regulators of stamen development in *Arabidopsis* identified by transcriptional profiling. Plant J. 2010;46(6):984-1008. https://10.1111/j.1365-313X.2006.02756.x.
4. Shikata M, Matsuda Y, Ando K, et al. Characterization of *Arabidopsis* ZIM, a member of a novel plant-specific GATA factor gene family. J Exp Bot. 2004;55(397):631-639.https://10.1111/j.1399-3089.2008.00478.x.
5. Yue W, Feng P, Danmei C, et al. Genome-wide identification and analysis of the *Populus trichocarpa* TIFY gene family. Plant Physiol Biochem. 2017;115(1):360-371. https://10.1016/j.plaphy.2017.04.015.
6. Howe G, Yoshida Y. Evolutionary origin of JAZ proteins and jasmonate signaling. Mol Plant. 2019;12(2):153-155.https://10.1016/j.molp.2019.01.015.
7. Boter M, Golz JF, Giménez-Ibañez SG, et al. FILAMENTOUS FLOWER is a direct target of *JAZ3* and modulates responses to jasmonate. Plant Cell. 2015;27(11):3160-3174.https://10.1105/tpc.15.00220.
8. Liu YY, Du MM, Deng L, et al. MYC2 regulates the termination of jasmonate signaling via an autoregulatory negative feedback loop. Plant Cell. 2019;31(1):106-127. https://10.1105/tpc.18.00405.
9. Chico JM, Chini A, Fonseca S, et al. JAZ repressors set the rhythm in jasmonate signaling. Curr Opin Plant Biol. 2008;11(5):486-494.https://10.1016/j.pbi.2008.06.003.
10. Muzaffar A, Chen YS, Lee HT, et al. A newly evolved rice-specific gene *JAUP1* regulates jasmonate biosynthesis and signalling to promote root development and multi-stress tolerance. Plant Biotechnol J. 2024;22(5):1417-1432.https://10.1111/pbi.14276.

11. Li Y, Tang JX, Qi YC, et al. Elevating herbivore-induced JA-Ile enhances potato resistance to the polyphagous beet armyworm but not to the oligophagous potato tuber moth. Pest Manag Sci. 2023;79(1):357-367. https://10.1002/ps.7205.
12. Huang H, Zhao WC, Qiao H, et al. *SlWRKY45* interacts with jasmonate-ZIM domain proteins to negatively regulate defense against the root-knot nematode *Meloidogyne incognita* in tomato. Hortic Res. 2022;9(1):3200-3212.https://10.1093/hr/uhac197.
13. Pan JW, Sohail H, Sharif R, et al. Cucumber JASMONATE ZIM-DOMAIN 8 interaction with transcription factor MYB6 impairs waterlogging-triggered adventitious rooting. Plant Physiol. 2024;197(1):1-18.https://10.1093/plphys/kiae351.
14. Toda Y, Tanaka M, Ogawa D, et al. RICE SALT SENSITIVE3 forms a ternary c omplex with JAZ and class-C bHLH factors and regulates jasmonate-induced gene expression and root cell elongation. Plant Cell. 2013;25(5):1709-1725.https://10.1105/tpc.113.112052.
15. Che L, Lu S, Gou H, et al. *VvJAZ13* positively regulates cold tolerance in *Arabidopsis* and grape. Int J Mol Sci. 2024;25(8):19-25.https://10.3390/ijms25084458.
16. Ma GM, Zhao KH, Zhang Y, et al. Dufulin-binding protein *OsJAZ5* functions in r ice stress toleranc. J Agric Food Chem. 2024;72(49):27094-27105.https://10.1021/acs.jafc.4c07852.
17. Zhao CY, Pan XW, Yu Y, et al. Overexpression of a TIFY family gene, *GsJAZ2*, exhibits enhanced tolerance to alkaline stress in soybean. Mol Breed. 2020;40(3):33-52.https://10.1007/s11032-020-01113-z.
18. Seo JS, Joo J, Kim MJ, et al. OsbHLH148, a basic helix-loop-helix protein, interacts with OsJAZ proteins in a jasmonate signaling pathway leading to drought tolerance in rice. Plant J. 2011;65(6):907-921.https://10.1111/j.1365-313X.2010.04477.x.
19. Onohata T, Gomi K. Overexpression of jasmonate-responsive *OsbHLH034* in rice r esults in the induction of bacterial blight resistance via an increase in lignin bios ynthesis. Plant Cell Rep. 2020;39(9):1175-1184. https://10.1007/s00299-020-02555-7.
20. Jiang Y, Yu D. The *WRKY57* transcription factor affects the expression of jasmonate ZIM-domain genes transcriptionally to compromise *Botrytis cinerea* Resistance. Plant Physiol. 2016;171(4):2771-2782.https://10.1104/pp.16.00747.

21. Mo HJ, Chang HM, Zhao G, et al. iJAZ-based approach to engineer lepidopteran pest resistance in multiple crop species. Nat Plants. 2024;10(5):771-784.https://10.1038/s41477-024-01682-3.

22. Chen SY, Zhang L, Ma QQ, et al. Jasmonate ZIM domain protein (JAZ) gene *SlJAZ15* increases resistance to *Orobanche aegyptiaca* in tomato. Plants. 2024;13(11):1493-1510.https://10.3390/plants13111493.

23. An JP, Xu RR, Xin L, et al. Jasmonate induces biosynthesis of anthocyanin and proanthocyanidin in apple by mediating the JAZ1–TRB1–MYB9 complex. Plant J. 2021;106(5):1414-1430. https://10.1111/tpj.15245.

24. Boyan T, Tan TT, Chen YT, et al. *SlJAZ10* and *SlJAZ11* mediate dark-induced leaf senescence and regeneration. PLoS Genet. 2022;18(7):e1010285.https://10.1371/journal.pgen.1010285.

25. Song S, Qi T, Huang H, et al. The Jasmonate-ZIM domain proteins interact with the R2R3-MYB transcription factors *MYB21* and *MYB24* to affect jasmonate-regulated stamen development in *Arabidopsis*. Plant Cell. 2011;23(3):1000-1013.https://10.1105/tpc.111.083089.

26. Wu NN, Zhang SF, Wang QH, et al. Fall webworm genomes yield insights into rapid adaptation of invasive species. Nat Ecol Evol. 2019;3(1):13-26. https://10.1038/s41559-018-0746-5.

27. Xu SJ, Zhang YQ, Li SC, et al. Plastid-expressed *Bacillus thuringiensis* (Bt) *cry3Bb* confers high mortality to a leaf eating beetle in poplar. Plant Cell Rep. 2020;39(3):317-323. https://10.1007/s00299-019-02492-0.

28. Plett JM, Daguerre Y, Wittulsky S, et al. Effector MiSSP7 of the mutualistic fungus *Laccaria bicolor* stabilizes the Populus JAZ6 protein and represses jasmonic acid (JA) responsive genes. Proc Natl Acad Sci USA. 2014;111(22):8299-8304.https://10.1073/pnas.1322671111.

29. Rao SP, Tian YR, Zhang C, et al. The JASMONATE ZIM-domain-OPEN STOMATA1 cascade integrates jasmonic acid and abscisic acid signaling to regulate drought tolerance by mediating stomatal closure in poplar. J Exp Bot. 2023;74(1):443-457. https://10.1093/jxb/erac418.

30. Wang HH, Wang XQ, Yu CY, et al. MYB transcription factor *PdMYB118* directly interacts with bHLH transcription factor PdTT8 to regulate wound-induced anthocyanin biosynthesis in poplar. BMC Plant Biol. 2020;20(1):173-187.https://10.1186/s12870-020-02389-1.

31. Yang GX, Wang SJ, Long LX, et al. Genome-wide identification and expression analysis of *PtJAZ* gene family in poplar (*Populus trichocarpa*). BMC Genom. Data. 2023;24(1):1-13.https://10.1186/s12863-023-01150-5.

32. Han Y, Luthe D.Identification and evolution analysis of the *JAZ* gene family in maize. BMC Genomics. 2021;22(1):256-277.https://10.21203/rs.3.rs-144271/v1.

33. Tong SF, Wang YB, Chen NN, et al. PtoNF-YC9-SRMT-PtoRD26 module regulate s the high saline tolerance of a triploid poplar. Genome Biol. 2022;23(1):148-176. https://10.1186/s13059-022-02718-7.

34. Yu XY, Lu B, Dong Y, et al. Cloning and functional identification of *PeWRKY41* from *Populus* × *euramericana*. Ind Crops Prod. 2022;175:114279.https://10.1016/j.indcrop.2021.114279.

35. Song HY, Duan ZH, Wang Z, et al. Genome-wide identification, expression pattern and subcellular localization analysis of the *JAZ* gene family in Toona ciliata. Ind Crops Prod. 2022;178(1):114582.https://10.1016/j.indcrop.2022.114582.

36. Yan W, Dong XM, Li R, et al. Genome-wide identification of *JAZ* gene family m embers in autotetraploid cultivated alfalfa (*Medicago sativa subsp*. sativa) and exp ression analysis under salt stress. BMC Genomics. 2024;25(1):636-654.https://10.1186/s12864-024-10460-6.

37.Shrestha K, Huang YH. Genome-wide characterization of the sorghum *JAZ* gene family and their responses to phytohormone treatments and aphid infestation. Sci Rep. 2022;12(1):32-48.https://10.1038/s41598-022-07181-9.

38. Jia K, Yan CY, Zhang J, et al. Genome-wide identification and expression analysis of the *JAZ* gene family in turnip. Sci Rep. 2021;11(1):1-13.https://10.1038/s41598-021-99593-2.

39. Tian SZ, Liu SY, Wang Y, et al. Genome-wide Identification and characterization of JAZ protein family in two petunia progenitors. Plants. 2019;8(7):203-215.https:/

/10.3390/plants8070203.

40. Wu W.Transcriptome-wide identification and characterization of the *JAZ* gene family in *Mentha canadensis* L.Int. J. Mol. Sci. 2021;22(16):8859.https://10.3390/ijms22168859.

41. Chen L, Wang P, Tan LX, et al. Genetic transformation of *Torenia fournieri* L. with the Bacillus thuringiensis *Cry1Ab* gene confers resistance to Mythimna separata (Walker). Plants-Basel. 2024;13(24):3568-3582.https://10.3390/plants13243568.

42. Paul W. Paré and James H. Tumlinson.Plant volatiles as a defense against insect herbivores.Plant Physiol. 1999;121(2):325-331.https://10.1104/pp.121.2.325.

43. Kaur R, Gupta AK, Taggar GK. Induced resistance by oxidative shifts in pigeonpea (*Cajanus cajan* L.) following *Helicoverpa armigera* (Hubner) herbivory. Pest Manag Sci. 2015;71(5):770-782.https://10.1002/ps.3851.

44. Zhu LC, Chen MS, Liu X. Changes in phytohormones and fatty acids in wheat and rice seedlings in response to hessian fly (*Diptera: cecidomyiidae*) Infestation. J Econ Entomol. 2011;104(4):1384-1392.https://10.1603/ec10455.

45. Rodriguez-Alvarez CI, Lopez-Climent MF, Gomez-Cadenas A, et al. Salicylic acid is required for Mi-1-mediated resistance of tomato to whitefly *Bemisia tabaci*, but not for basal defense to this insect pest. Bull Entomol Res. 2015;105(5):574-582. https://10.1017/S0007485315000449.

46. Onkokesung N, Reichelt M, Wright LP, et al. The plastidial metabolite 2-C-methyl-D-erythritol-2,4-cyclodiphosphate modulates defence responses against aphids. Plant Cell Environ. 2019;42(7):2309-2323.https://10.1111/pce.13538.

47. Liu JL, Du HT, Ding X, et al. Mechanisms of callose deposition in rice regulated by exogenous abscisic acid and its involvement in rice resistance to *Nilaparvata lugens* Stal (Hemiptera: Delphacidae). Pest Manag Sci. 2017;73(12):2559-2568.https://10.1002/ps.4655.

48. Zhang YJ, Yun XH, Wang HR, et al. SlMYC2 interacted with the *SlTOR* promoter and mediated JA signaling to regulate growth and fruit quality in tomato. Front Plant Sci. 2022;13(1):1013445.https://10.3389/fpls.2022.1013445.

49. Zhang LL, Huang YY, Zheng YP, et al. Osa-miR535 targets SQUAMOSA promot

er binding protein-like 4 to regulate blast disease resistance in rice. Plant J. 2022; 110(1):166-178.https://10.1111/tpj.15663.

50. Lu L, Sun Z, Wang R, et al. Integration of transcriptome and metabolome analyses reveals the role of *OsSPL10* in rice defense against brown planthopper. Plant Cell Rep. 2023;42(12):2023-2038.https://10.1007/s00299-023-03080-z.

51. Feuillet C, Travella S, Stein N, et al. Map-based isolation of the leaf rust disease resistance gene *Lr10* from the hexaploid wheat (*Triticum aestivum* L.) genome. Proc Natl Acad Sci USA. 2004;100(25):15253-15258.https://10.1073/pnas.2435133100.

52. Kandoth PK, Ranf S, Pancholi SS, et al. Tomato MAPKs LeMPK1, LeMPK2, and LeMPK3 function in the systemin-mediated defense response against herbivorous insects. Proc Natl Acad Sci USA. 2007;104(29):12205-12210.https://10.1073/pnas.0700344104.

53. Han LB, Li YB, Wang HY, et al. The dual functions of WLIM1a in cell elongation and secondary wall formation in developing cotton fibers. Plant Cell. 2013;25(11):4421-4438.https://10.1105/tpc.113.116970.

54. Wang XP, Xiang YJ, Sun MS, et al. Transcriptomic and metabolomic analyses rev eals keys genes and metabolic pathways in tea (*Camellia sinensis*) against six-spot ted spider mite (*Eotetranychus Sexmaculatus*). BMC Plant Biol. 2023;23(1):16-27.h ttps://10.1186/s12870-023-04651-8.

55. Chen XH, Su WL, Zhang H, et al. *Fraxinus mandshurica* 4-coumarate-CoA ligase 2 enhances drought and osmotic stress tolerance of tobacco by increasing conifery l alcohol content. Plant Physiol Biochem. 2020;155(1):697-708.https://10.1016/j.plap hy.2020.08.031.

56. Zhang GY, Zhang YJ, Xu JT, et al. The *CCoAOMT1* gene from jute (*Corchorus capsularis* L.) is involved in lignin biosynthesis in *Arabidopsis thaliana*. Gene. 2014;546(2):398-402.https://10.1016/j.gene.2014.05.011.

Supplementary Files

This is a list of supplementary files associated with this preprint. Click to download.

- Supplementary.docx